Multidisciplinary study of the Lower Palaeolithic site of Cimitero di Atella (Basilicata), Italy

Roxane Rocca, Paolo Giannandrea, Alison Pereira, Jean-Jacques Bahain, Francesco Boschin, Amélie Da Costa, Federico Di Rita, François Fouriaux, Alessio Iannucci, Lucie Germond, et al.

Multidisciplinary study of the Lower Palaeolithic site of Cimitero di Atella (Basilicata), Italy

4XDWHUQDU\ ,QWHUQDWLRQDO 0XOWLGLVFLSOLQDU\ VWXG\ RI WKH /RZHU 3DODHROL ,WDO\

0DQXVFULSW 'UDIW

0DQXVFULSW 1XPEHU	
$UWLFOH 7\SH	5HJXODU $UWLFOH
&RUUHVSRQGLQJ $XWKRU	5R[DQH 5RFFD 8QLYHUVLW« 3DULV , 3DQWK«RQ 6RUERQQH 3DULV •OH GH)UDQFH)5$1&(
)LUVW $XWKRU	5R[DQH 5RFFD
2UGHU RI $XWKRUV	5R[DQH 5RFFD
	3DROR *LDQQDQGUHD
	$OLVRQ 3HUHLUD
	-HDQ -DFTXHV %DKDLQ
	)UDQFHVFR %RVFKLQ
	$P«OLH 'D &RVWD
	)HGHULFR 'L 5LWD
	)UDQ©RLV)RXULDX[
	$OHVVLR ,DQQXFFL
	/XFLH *HUPRQG
	'DULR *LRLD
	'RQDWHOOD 0DJUL
	%HQLDPLQR 0HFR]]L
	6HEDVWLHQ 1RPDGH
	5DIIDHOH 6DUGHOOD
	0DUFHOOR 6FKLDWWDUHOOD
	3LHUUH 9RLQFKHW
	'DQLHOH $XUHOL
$EVWUDFW	7KH /RZHU 3DODHROLWKLF VLWH RI &LPLWHUR GL $WHOO 6RXWKHUQ ,WDO\ DERXW NP VRXWK RI WKH H[WLQFW GLVFRYHUHG LQ WKH HDUO\ V DQG ZDV FRQWLQXRXVO XQGHU WKH VXSHUYLVLRQ RI 3URIHVVRU (%RU]DWWL YR 7KLV RSHQ DLU VLWH FRQWDLQHG D ILYH PHWUH WKLFN I E\ WKH RFFXUUHQFH RI WZR PDLQ DUFKDHRORJLFDO XQLW UHPDLQV %DVHG RQ WKH FRPSRVLWLRQ RI WKH OLWKLF SUHVHQFH RI KDQGD[HV LQ WKH /RZHU XQLW %RU]DWWL DWWULEXWHG WKH VLWH WR WKH (DUO\ $FKHXOHDQ &LPL UHVXOW RI YDULRXV ODNH VKRUH RFFXSDWLRQV OLQNHG 3DODHROR[RGRQ DQWLTXXV DQG %LVRQ VS DQG WKH R SURGXFH VLPSOH VPDOO DQG ODUJH OLWKLF WRROV %RU 7KH SXUSRVH RI WKLV SDSHU LV WR SUHVHQW WKH ODVW *HRFKURQRORJLFDO SDODHRQWRORJLFDO DQG SDO\QRO FRQGXFWHG WR VKHG OLJKW RQ WKH HQYLURQPHQWDO D WKH DVVRFLDWHG KXPDQ RFFXSDWLRQV OHYHOV 7KLV IL HYDOXDWH WKH QDWXUH DQG SRWHQWLDO RI DUFKDHROR D EURDGHU IUDPHZRUN
6XJJHVWHG 5HYLHZHUV	0DUWD $U]DUHOOR

	U]UPUW#XQLIH LW
	%LDJLR *LDFFLR ELDJLR JLDFFLR#FQU LW
	-HDQ /XF *XDGHOOL MHDQ OXF JXDGHOOL#X ERUGHDX[IU
	0D JRU]DWD .RW P NRW#XZ HGX SO
	/DXUHQW 'HVFKRGW ODXUHQW GHVFKRGW#LQUDS IU

Roxane ROCCA

Maîtresse de conférence
Université Paris 1 (Panthéon-Sorbonne)
Institut d'Histoire de l'Art et d'Archéologie
3, rue Michelet F-75005 Paris
UMR 8068 – TEMPS (Technologie et Ethnologie des Mondes PréhistoriqueS)
MSH Mondes, Bâtiment René Ginouvès,
21 Allée de l'Université, F-92023 Nanterre.
Roxane.rocca@univ-paris1.fr

Cover letter to Quaternary International

Paris,13/02/2023

Dear Editor,

I have the honour to submit, on behalf of all the collaborators, this article entitled "Multidisciplinary study of the Lower Palaeo
This is a first synthetic work on the Lower Palaeolithic site of Cimitero di Atella in Italy. We resumed excavation on the site in 2016 and carried out new studies on the archaeological material, but also on the environmental context and the chronostratigraphic framework. Roxane ROCCA and Daniele AURELI have the excavation permit from the Italian Heritage and manage the field organisation and documentation together with Lucie GERMOND, Amélie DA COSTA and François FOURIAUX. Roxane ROCCA, Daniele AURELI, Lucie GERMOND and Amélie DA COSTA participate to the lithic study. Paolo GIANNANDREA, Dario GIOIA and Marcello SCHIATTARELLA, conducted the geological study, Alison PEREIRA and Sebastien NOMADE the Ar/Ar dating, Jean-Jacques BAHAIN and Pierre VOINCHET the ESR dating. The archaeozoological and palaeontological study was led by Francesco BOSCHIN, Alessio IANNUCCI, Beniamino MECOZZI and Raffaele SARDELLA. Donatella MAGRI and Federico DI RITA where in charge of the palynological analysis. All the co-author to the article produced the figures and text corresponding to their skill and have approved the final version of the manuscript.
Hoping that this article will be of interest to your review.
Best regards,
Roxane ROCCA

Multidisciplinary study of the Lower Palaeolithic site of *Cimitero di Atella* (Basilicata), Italy.

Roxane ROCCA[a], Paolo GIANNANDREA[b], Alison PEREIRA[c], Jean-Jacques BAHAIN[d], Francesco BOSCHIN[e], Amélie DA COSTA[f], Federico DI RITA[g], François FOURIAUX[h], Alessio IANNUCCI[i], Lucie GERMOND[j], Dario GIOIA[k], Donatella MAGRI[l], Beniamino MECOZZI[i], Sebastien NOMADE[m], Raffaele SARDELLA[i], Marcello SCHIATTARELLA[b], Pierre VOINCHET[d], Daniele AURELI[n].

a. Université Paris 1 Panthéon-Sorbonne, école d'histoire de l'archéologie de la Sorbonne, UMR 8068, Technologie et Ethnologie des Mondes PréhistoriqueS (TEMPS), MSH Mondes, Bâtiment René Ginouvès, 21 Allée de l'Université, 92023 Nanterre Cedex, France. roxane.rocca@univ-paris1.fr

b. Dipartimento delle Culture Europee e del Mediterraneo, Università della Basilicata, via Lanera, 20 – 75100 Matera, Italy. paolo.giannandrea@unibas.it marcello.schiattarella@unibas.it

c. Université Paris-Saclay, Umr 8148 GEOPS, Campus de l'Université Paris Sud Bâtiment 504, Rue du Belvédère, 91405 Orsay Cedex, France. alison.pereira@universite-paris-saclay.fr

d. Muséum national d'Histoire naturelle de Paris, Département « Homme et Environnement », UMR7194, Histoire Naturelle de l'Homme Préhistorique (HNHP), 1 rue René Panhard, 75013, Paris, France. jean-jacques.bahain@mnhn.fr pierre.voinchet@mnhn.fr

e. Università Degli Studi di Siena, Dipartimento di Scienze Fisiche, Della Terra e Dell'Ambiente, UR Preistoria e Antropologia, Via Laterina 8, IT 53100, Siena, Italy. boschin@unisi.it

f. Service départemental d'archéologie du Val d'Oise, UMR 7041, ArScAn, Equipe AnTET, MSH Mondes, Bâtiment Max Weber, 21 Allée de l'Université, 92023 Nanterre Cedex, France. amel.dacosta@gmail.com

g. Dipartimento di Biologia Ambientale, Sapienza Università di Roma, Piazzale Aldo Moro 5,

00185 Roma, Italy. federico.dirita@uniroma1.it donatella.magri@uniroma1.it

h. Centre Jean Bérard, École française de Rome, UMR 8546 AOROC, Campus Condorcet, Bâtiment Recherche Nord, 14 Cours des Humanités, 93322 Aubervilliers, France. francois.fouriaux@cnrs.fr

i. Department of Earth Sciences (PaleoFactory lab.), Sapienza University of Rome, Piazzale Aldo Moro 5, 00185, Rome, Italy. alessio.iannucci@uniroma1.it beniamino.mecozzi@uniroma1.it raffaele.sardella@uniroma1.it

j. lucie.germond@hotmail.fr

k. CNR-ISPC, Tito Scalo, 85050, Potenza, Italy. dario.gioia@cnr.it

m. CEA-CNRS, UMR 8212, Laboratoire des Sciences du Climat et de l'Environnement, CEA-UVSQ et Université Paris Saclay, Bat 714, Orme des Merisiers, 91191 Gif sur Yvette, France. LSCE sebastien.nomade@lsce.ipsl.fr

n. UMR 7041, ArScAn, Equipe AnTET, MSH Mondes, Bâtiment Max Weber, 21 Allée de l'Université, 92023 Nanterre Cedex, France. danieleaureli1@gmail.com

Abstract:

The Lower Palaeolithic site of Cimitero di Atella is located in the Basilicata region (Southern Italy), about 10 km south of the extinct Monte Vulture volcano. The site was discovered in the early 1990s and was continuously excavated for nearly twenty years under the supervision of Professor E. Borzatti von Löwenstern (University of Florence). This open-air site contained a five-metre-thick fluvio-lacustrine sequence characterized by the occurrence of two main archaeological units with lithic industries and faunal remains. Based on the composition of the lithic assemblages, and in particular the presence of handaxes in the Lower unit, Borzatti von Löwenstern (et al., 1997) attributed the site to the Early Acheulean. Cimitero di Atella was interpreted as the result of various lake shore occupations linked to the exploitation of large mammals (*Palaeoloxodon antiquus* and *Bison* sp.) and the opportunistic use of raw materials to produce simple small and large lithic tools (Borzatti von Löwenstern et al., 1997).

The purpose of this paper is to present the last five years of research at the site. Geochronological, palaeontological and palynological investigations have been conducted to shed light on the environmental and chronological context of the site and the associated human occupations levels. This first essential step enables us to evaluate the nature and potential of archaeological data in order to place the results in a broader framework.

Keywords:

Lower Palaeolithic, Quaternary, Monte Vulture Volcano, Geology, Geochronology, 40Ar/39Ar geochronology, Lithic industry, Early–Middle Pleistocene Transition (EMPT)

1. Introduction

The Lower Palaeolithic site of Cimitero di Atella is located in the Basilicata region (Southern Italy), about 10 km south of the extinct Monte Vulture volcano (Figure 1). The site was discovered in the early 1990s and was continuously excavated for nearly twenty years under the supervision of Professor E. Borzatti von Löwenstern (University of Florence). This open-air site contained a five-metre-thick fluvio-lacustrine sequence characterized by the occurrence of two main archaeological units with lithic industries and faunal remains. Based on the lithology of the sedimentary layers and biochronological information from the faunal assemblages, the site was confidently attributed to the Middle Pleistocene timescale (Borzatti von Löwenstern et al., 1990; Ciolli, 1997; Di Muro, 1999; Zucchelli, 2002). The presence of volcanic materials (tephra, ignimbrites and reworked volcanic minerals found in the fluvial deposits) typical of the early explosive activity of the Monte Vulture volcano indicates that human occupation took place between about 740 ka and 480 ka (Di Muro, 1999). Based on the composition of the lithic assemblages, and in particular the presence of handaxes in the Lower unit, Borzatti von Löwenstern (et al., 1997) attributed the site to the Early Acheulean. Cimitero di Atella was interpreted as the result of various lake shore occupations linked to the exploitation of large mammals (*Palaeoloxodon antiquus* and *Bison* sp.) and the opportunistic use of raw materials to produce simple small and large lithic tools (Borzatti von Löwenstern et al., 1997).

In the light of increased early Acheulean evidence over the past decade (García-Medrano et al.,

2014; Moncel et al., 2016, 2019; Mosquera et al., 2016), as well as the still-open debate on the modes and temporality of the emergence of handaxes in Europe (Moncel and Schreve, 2016; Moncel et al., 2018; Nicoud, 2013; Rocca et al., 2016a), Cimitero di Atella is of particular interest. The presence of handaxes and large cutting-tools before 0.5 Ma is now well attested, mainly in South-western Europe. This is generally explained by a second wave of settlement originating from Africa driving classical Acheulean development. In many respects, this hypothesis is still tenuous as available data are still scarce for this pivotal period in Europe, between early settlement and the classical Acheulean. Moreover, the comprehensive interpretation of settlement dynamics during this period is difficult, given the diversity of archaeological contexts (cave, palimpsest, snapshot, etc…), as well as the plurality of lithic methodological approaches. In this background, the site of Cimitero di Atella will undoubtedly help to test the various hypotheses concerning the diffusion of the Acheulean in Europe.

At the end of Borzatti von Löwenstern excavation at the site, many questions were still pending. First of all, the chronological attribution based on volcano-stratigraphic correlation required confirmation by sedimentological analysis and radiometric dating. Secondly, the question of site formation dynamics was crucial to interpret the archaeological record and assess the different taphonomic aspects. Finally, it was indispensable to study the archaeological material with a methodology adapted to topical issues in order to compare it to other contemporaneous sites.

A new multidisciplinary research project was thus launched at Atella in 2015, aiming to understand the site infilling and to clarify the archaeological context of the sequence. This work was rendered possible by the advancement of stratigraphic and palaeoenvironmental research on Middle Pleistocene volcanic and epiclastic successions outcropping at the Monte Vulture volcano and in the adjacent Atella and Venosa fluvio-lacustrine basins (Schiattarella et al., 2005; Giannandrea et al., 2006; Giannandrea, 2009; Schiattarella et al., 2016). New excavation campaigns were carried out and the material (lithic and fauna) preserved in the Melfi Museum collection was re-studied.

The purpose of this paper is to present the last five years of research at the site. Geochronological, palaeontological and palynological investigations have been conducted to shed light on the

environmental and chronological context of the site and the associated human occupations levels. This first essential step enables us to evaluate the nature and potential of archaeological data in order to place the results in a broader framework.

2. Regional setting

2.1 History of research at Atella

Since the end of the nineteenth century, the Monte Vulture region, and in particular the Venosa and Atella basins (see SM1).

Since the 2000s, research focused on the upper part of the stratigraphy, and revealed an alluvial environment with a high composition of volcanoclastic sediments (Borzatti von Löwenstern, 2011). In parallel, Borzatti von Löwenstern's team installed explanatory panels around the site and published a series of books geared towards the general public (Borzatti von Löwenstern, 1985; Borzatti von Löwenstern and Sozzi, 2001). The systematic excavation by the Florentine research group ended in 2012.

Renewed interest in the non-bifacial component of Lower Palaeolithic lithic industries led to a technological and techno-functional study of all the lithic industries from level F of the Atella site (Abruzzese, 2014). From 2017 to 2021, research at Atella was mainly funded by the École française de Rome as part of a larger programme on settlement dynamics during the Lower Palaeolithic in Italy (Rocca et al., 2018, 2020; Rocca and Aureli, 2019). Currently, the site of Atella is part of a valorization project funded by local and European institutions.

2.2 Geological context

The study area is in a volcanic district of Southern Italy, characterized by a complex stratigraphy of interbedded pyroclastic and sedimentary deposits spread over a 750 km^2 area along the external (i.e., north-eastern) sector of the Apennines chain (Figure 2, a). More precisely, the *Cimitero di Atella* site is located at the top of the fluvial-lacustrine succession of the Atella Basin (Giannandrea et al., 2006), about 10 km south of the Monte Vulture volcano (Figure 2, b).

130 The volcanic sequence has been subdivided into unconformity-bounded stratigraphic units
131 (UBSU), in turn grouped into two Middle Pleistocene Supersynthems, labelled Monte Vulture and
132 Monticchio (Tab. 1). The Monte Vulture Supersystem includes the products of the central volcano
133 (subdivided into the Foggianello, Barile, and Melfi synthems), the underlying alluvial sediments, and
134 the fluvial-lacustrine infill of the Atella and Venosa basins (Figure 2), whereas the Monticchio
135 Supersynthem comprises products correlated to some small eruptive vents. The age of the Monte
136 Vulture Supersynthem ranges from 698 ± 8 ka to 573 ± 4 ka, whereas the time-span of the Monticchio
137 Supersynthem is between 494 ± 5 ka and 141 ± 11 ka (Giannandrea et al., 2006; Villa and Buettner,
138 2009).
139 The lacustrine silty-sandy clay and the heteropic alluvial conglomerate of the Atella Basin i) cover
140 the ignimbrite deposits of the Fara d'Olivo Subsynthem (Table 1), ii) are correlated with the
141 pyroclastic and fall deposits of the Rionero Subsynthem, and iii) are covered by lava and pyroclastic
142 flows of the Vulture - San Michele Subsynthem (Giannandrea et al., 2014; Schiattarella et al., 2016;
143 Table 1). The latter are overlain by epiclastic deposits of the Piana del Gaudo and by travertines of
144 Atella village. (Figure 3).

145 ## 3. Material and methods

146 The new research on the Palaeolithic site of Cimitero di Atella begin in 2014 after excavations by
147 the Borzatti von Löwenstern team had stopped. In this section we will present the material studied in
148 this paper and the methods employed. These include excavation methods in the field, geological,
149 geochronological and palaeoenvironment data, and the sampling and study methods applied to faunal
150 and lithic remains.

151 ### 3.1. Excavation method

152 The excavation strategy had to take into account constraints linked to the state of preservation of
153 the site. During the initial excavation years in the early 1990s, the Borzatti von Löwenstern team
154 decide to build a first protective cover. It consisted of a roof covering the excavation area, supported

155 by a first module made of metal tubes. Then, over the following years, a series of interventions were
156 carried out. The covered surface was extended towards the cemetery wall, in order to increase the
157 excavation surface. When the new research project began in 2015, the site was therefore covered by
158 the metallic protective structure (SM2a) and included more than 2 metres section limiting the
159 excavation possibilities. Moreover, as some archaeological finds were still exposed on the excavation
160 surface, in 2015 we first of all focused on the restoration and when possible the recording of finds.
161 During these two preliminary years of the project, we concentrated in particular on the revaluation of
162 the chronostratigraphic context, by drilling two cores, one from each side of the site, and collecting
163 samples for radiometric dating. In 2016, 2017 and 2018, we began the excavation of several square
164 metres in the F levels inside the Borzatti von Löwenstern area, and in 2019 we opened a new 25 m^2
165 area to the east of the former excavation (Figure 4). In 2020, we were able to enlarge the excavation
166 area owing to a project promoting archaeology led by the Atella municipality. The Borzatti von
167 Löwenstern protective structure was dismantled and a new area was opened with mechanical diggers.
168 The excavation area is now 250 m^2 and includes the Borzatti von Löwenstern area and the 2019 area
169 (Figure 4), which is now covered by a new adapted covering roof.
170 In each geological unit, the archaeological excavation proceeded by artificial levels of 5 cm, per
171 quarter of a square metre, in order to locate the small elements found in the sediments during sieving.
172 The three coordinates (x, y, z), the direction, dip and dip angle were recorded for all remains larger
173 than 1 cm. The exploitation of these data is still in progress, and together with the micromorphological
174 analysis, will provide information on the formation process of the levels.

175 3. 2. Geology

176 The stratigraphy of the exposed sediments of the Cimitero di Atella site was studied and the
177 sediments from the drilling cores were analysed (Figure 4a). The detailed sedimentological analysis,
178 which took into account grain size, sorting, and primary sedimentary structures, brought to light a
179 series of lithofacies grouped into two associations, briefly described in Table 2. The facies were
180 determined and interpreted on the basis of papers by Miall (1978), Walker and James (1992), Fisher

and Schmincke (1994), Sanders et al. (2009), Nehyba and Nývlt (2014), and Palladino et al., (2018). In addition, some layers were sampled for palynological and geochronological analyses. In order to establish lateral stratigraphic correlations between the deposits from the Cimitero di Atella site and the Monte Vulture sequence, we performed a detailed field survey in the Atella village area, studying a topographic profile across the Atella plateau and drilling two cores (Figure 3, Figure 4a). From a geomorphological viewpoint, the investigated site is located on a flat-topped hill, overlain by travertine deposits. A straight scarp crosses this sub-horizontal land surface, due to the presence of a high-angled normal fault cutting into the entire succession (Figure 5).

3. 3. Dating

Four sedimentary layers (Figure 6), labelled Atella INF (ash flow deposit Tng, 5 m below the archaeological excavation), F, I and L2, were dated by $^{40}Ar/^{39}Ar$ on single grains at Cimitero di Atella. In addition, two levels, L1 and L3 (Figure 6), were sampled for ESR dating of optically-bleached quartz grains.

3.3.1. $^{40}Ar/^{39}Ar$

The samples were crushed and sieved, and crystals were extracted from the 500-250 μm fraction size. They were then cleaned in distilled water using an ultrasonic bath. Unaltered and pristine potassic feldspars (mainly sanidines) were then handpicked under a binocular microscope and leached with a 7 % HF solution for about 5 minutes to remove potential particles and alteration phases from the surface of minerals. Thirty to fifty crystals were selected to be irradiated. They were loaded into aluminium discs. Prior to mass spectrometric measurements, samples were activated in two distinct irradiations. All the samples were irradiated in the β1 tube of the Osiris reactor (French Atomic Energy Commission, Saclay France). Sample Atella INF was irradiated for 60 min (IRR 99) while samples F, I and L2 were irradiated for 90 min (IRR 108). Interference corrections were based on the nucleogenic production ratios given in Guillou et al. (2018) for Osiris. After irradiation, crystals were transferred into a copper sample holder and individually loaded into a differential vacuum Cleartan© window. The analytical procedure is described in detail in Nomade et al. (2010). Minerals were fused

one by one using a 25 Watts Synrad CO2 laser at about 10 to 15 % of nominal power. The extracted gases were then purified for 10 min by two hot GP 10 and two GP 50 getters (ZrAl). Argon isotopes (40Ar, 39Ar, 38Ar, 37Ar and 36Ar) were successively measured using a VG 5400 mass spectrometer equipped with an electron multiplier (Balzer SEV 217 SEN). Each argon isotope measurement consisted of 20 cycles of peak-hopping. Neutron fluence J for each sample was calculated using co-irradiated Alder Creek sanidine standard (ACs at 1.1891 Ma, optimization calibrated age of Niespolo et al., 2017) and the 40K total decay constant of Renne et al., 2011). For the two irradiations (IRR 99 and 108), J-values were computed from a monitor co-irradiated with each dated sample (Atella INF: J = 0.000396998 ± 0.00000199; F: J = 0.00039550 ± 0.00000159; I: J = 0.00038743 ± 0.00000155. L2: J = 0.0004186 ± 0.00000029). Mass discriminations were monitored by the analysis of air pipettes throughout the analytical period, and relative to a $^{40}Ar/^{36}Ar$ ratio of 298.56 (Lee et al., 2006). Procedural blank measurements were taken after every two or three unknown samples. For a typical 10-minute duration of isolation, typical backgrounds are about 2.0-3.0 x 10-17 and 5.0 to 6.0 x 10-19 moles for 40Ar and 36Ar, respectively.

3.3.2. ESR on bleached quartz

ESR analyses of quartz grains were performed using the multi-centre approach, based on the measurement of both aluminium (Al) and titanium-lithium (Ti-Li) centres in a given quartz sample (Toyoda et al., 2000; Tissoux et al., 2007). Indeed, these two ESR centres display different behaviours with regard to light on the one hand and irradiation on the other hand. Ti-Li centres are quickly and totally bleached by solar light (in a few days), and are also much more radiosensitive than Al centres, and saturate under irradiation much faster than the latter (Duval and Guilarte, 2015). In contrast, Al centres are very stable under irradiation but are not totally reset even after long light exposure (several months). Therefore, a more complex protocol is required to determine the unbleachable part of the dated quartz grains (Voinchet et al., 2004).

Firstly, the quartz grains were extracted from the samples using the chemical and physical protocol described by Voinchet et al. (2020). After extraction, each purified quartz sample was split into eleven aliquots. Nine of them were irradiated with a γ 60Co source (Commissariat à l'Énergie Atomique,

Saclay, France) at doses ranging from 264 to 12,500 Gy. One aliquot was conserved as a natural reference and the eleventh aliquot was exposed during 1,600 h to light in a Dr Honhle© SOL2 solar simulator (light intensity between 3.2 and 3.4 105 Lux) in order to determine the unbleachable portion of the ESR-Al signal. Each sample set of eleven aliquots was measured at least three times by ESR at 107K using a Bruker© EMX spectrometer and every measure of each aliquot was undertaken three times after an approximatively 120° rotation of the tube in the ESR cavity, in order to consider angular dependence of the signal due to sample heterogeneity. The ESR acquisition parameters used were 5 mW microwave power, 1024 point resolution, 20 mT sweep width, 100 kHz modulation frequency, 0.1 mT modulation amplitude, 40 ms conversion time, 20 ms time constant and 1 scan.

Signal intensity was then measured between the top of the first peak at g=2.018 and the bottom of the 16th peak at g=2.002 of the Aluminium hyperfine structure and by measuring the difference between the peak top (g= 1.913) of the Ti-Li signal and the baseline (Toyoda and Falguères, 2003). Equivalent doses (DE) were then determined from the obtained ESR intensities versus the dose growth curves using a coupled exponential and linear function with Microcal OriginPro 8 software with $1/I^2$ weighting (Voinchet et al., 2020).

External alpha and beta contributions to the dose rate were obtained using the dose-rate conversion factors of Guérin et al. (2011) from the sediment radioelement contents (U, Th and K) measured in the laboratory by high-resolution and low background gamma-spectrometry (Table 3). Gamma dose rate was determined by in situ measurements with an Inspector 1000 (Canberra©) gamma spectrometer (Canberra©) using the threshold method (Mercier and Falguères, 2007). A k-value of 0.15 ± 0.1 (Laurent et al., 1998), alpha and beta attenuations from Brennan (2003) and Brennan et al. (1991), sediment water content estimated from the difference in mass between the natural sample and the same sample dried in an oven at 40°C for a week and water attenuation formulae from Grün (1994) were used in the age calculation. The cosmic dose rate was estimated from the equations of Prescott and Hutton (1994). The internal dose rate was considered to be negligible because of the low radionuclide content usually found in quartz grains.

3. 4. Fauna

A preliminary identification was carried out on 621 faunal remains stored at the Heritage Office in the Castle of Melfi (PZ). These remains are from Borzatti von Löwenstern's fieldwork and the new excavations carried out in 2015 and 2016. Most of the identifications are limited to the taxonomic family or genus. Further work will attempt to refine the taxonomy of faunal remains from Atella. A taphonomic approach was applied to a subsample, excluding specimens with modern fractures, or incrusted by concretions. Specimen size was considered for 585 specimens, and the state of preservation was observed on 600 remains. In particular, considering the geological setting of the site, we classified specimens according to their level of rounding: i) specimens with no rounding; ii) specimens with slightly rounded edges; iii) specimens with rounded edges or completely reshaped by agents of transport (probably water).

3. 5. Palynology

Fourteen samples were taken from core 2 of Cimitero di Atella for pollen analysis, from the following depths: 5.60, 6.80, 9.20, 9.60, 10.80, 11.20, 12.03, 12.40, 12.80, 13.20, 13.60, 14.02, 14.40, and 14.80 m. They were chemically treated with HCl (37%), HF (40%) and NaOH (10%) according to standard procedures for pollen extraction summarized in Magri and Di Rita (2015). Pollen concentrations were determined by adding tablets of spores of exotic *Lycopodium* to known weights of sediment. Observations were carried out by means of a light microscope at ×400 magnifications. For each sample, at least two slides were prepared and analysed.

Unfortunately, all the samples, excluding the sample at 14.02 m, were barren. In the sample at 14.02 m, after a series of three analysed slides, only one pollen grain of Poaceae was counted, which is clearly insufficient to define the past vegetation of the site. The lack of pollen grains can be ascribed to problems of pollen preservation, a very high sedimentation rate which would have diluted the pollen content within the sediment, or barren vegetation due to harsh glacial conditions. However, it is also likely that all these factors contributed to the absence of pollen.

3. 6. Lithic artefacts

The studied corpus is from the previous excavation led by Borzatti von Löwenstern and from the new 2015 to 2018 excavations (Table 4). The old collection contains two main assemblages, excluding surface finds, one from Level L, the other from Level F. Given the disparate states of alteration, and some doubts concerning the anthropic nature of several pieces, only the more reliable items were selected (Abruzzese et al., 2016). The following criteria were retained to improve the reliability of the assemblage: type of blank and raw material, the degree of alteration, the type of patina and the presence of a double patina, and the presence or absence of knapping scars. We subdivided the material into three groups, definite non-anthropic items, probable poorly-preserved anthropic elements, and anthropic items. Only the last group was analysed. In level L, only 107 pieces were selected out of 2553 (Borzatti von Löwenstern, 2005), and 666 of the 7887 pieces from level F (Abruzzese et al., 2016).

Raw materials can be divided into three types: flint, quartzite and a highly altered raw material, described as “porous radiolarite” (Borzatti von Löwenstern et al., 1997), which is probably a fine limestone.

A technological approach was applied to the lithic assemblage of Atella (Boëda et al., 1990; Inizan et al., 1999; Boëda, 2013), in order to describe the reduction sequence (selection, production aims, use, management, etc.). In this paper, we focus on the production phase and the identification of the main technological categories: cores, debitage flakes, small tools, large tools, retouch flakes, based on the diacritical scheme of each piece (chronology and direction of removal, measurements, angles, etc.). We also began to analyse some piece with a techno-functional analysis (Lepot, 1991; Boëda, 2013; Aureli et al., 2016; Rocca et al., 2016) in order to identify the transformative and prehensile part of the tools.

4. Results

4. 1. Stratigraphic and sedimentological analysis

The horizontally-bedded Quaternary succession outcropping in the study area unconformably overlies the sedimentary bedrock, represented here by Numidian Flysch (age: Burdigalian – Langhian?). Miocene sediments only outcrop to the east of Atella village (Figure 3) and consist of tilted quartzarenite beds. The Quaternary sequence of the site (Figure 6) is formed, from the base, of light-grey horizontally-laminated volcaniclastic siltstone of the **Sh** lithofacies (Figure 7 and Figure 7a), attributed to sediment decantation in a lacustrine environment. Toward the north, such sediments are in heteropic relationships with volcaniclastic alluvial conglomerates (Figure 3a). Above them, a lava flow and pyroclastic and epiclastic deposits, labelled 3a, 3b and 4 in Figure 3, and swamp and alluvial deposits, are recorded in the surveyed area. Finally, the travertine of Atella village (Figure 3) unconformably overlies the previously described deposits, through an erosive surface.

In the Cimitero di Atella site, at the top of facies **Sh**, the base of the stratigraphic succession (Figure 6) is composed of horizontal beds of the **TLm** lithofacies (Figure 7b), interpreted as pyroclastic ash flow deposits, with intercalations of fallout ash deposits, attributed to lithofacies **Tng** (Figure 7c) and **Tm** (Figure 7d). Laterally (i.e., towards the north and to the west of Atella village), the pyroclastic beds overlie a lava flow (Figure 3) attributed to the Vulture - San Michele Subsynthem by Giannandrea et al. (2006). Moving up, about 2-m-thick lacustrine deposits of lithofacies **Sh**, **Dh**, and **Su** (Figure 8a) are overlain by two epiclastic breccia (Figure 7e) with volcanic clasts (lithofacies **Bmli)**, connected to cohesive debris flow. Each breccia layer is covered by reworked sediments of the **Suli** lithofacies (Figure 7e). Both lithofacies **Bmli** and **Suli** contain lithic industry and two tusks of *Palaeoloxodon antiquus* (Borzatti von Löwenstern et al., 1997). A westward-dipping erosive surface is present at the top of these sediments (Figure 7).

The upper portion of the succession is characterized by alternating beds of primary volcanic deposits – made up of ash and lapilli fallout from lithofacies **Tm** and **Lm** (Figure 8d) and pyroclastic flow from lithofacies **LTm** (Figure 8b), **TLm**, and **TLBm** (Figure 8c) – and trough cross-bed

334 epiclastic volcanic sediments corresponding to lithofacies **SBt** and **Sr** (Figure 8b and Figure 8d). It is
335 noteworthy that **Lm** and **SBt** facies are frequently associated in the same horizon. Often, the beds at
336 the base of lithofacies **LTm**, **TLm**, **TLBm**, and **Bmli** show water-escape pipes. These are soft-
337 sediment deformation structures due to the unstable density of the water-saturated alluvial (Figure 8c
338 and Figure 8d) and lacustrine (Figure 8) sediments. Here, such structures can be interpreted as loading
339 structures resulting from the rapid sedimentation of mass deposits (Anketell et al., 1969).
340 This suggests that the deposition of facies **Bmli** occurred immediately after the lake was drained,
341 when sediments were still saturated. Is also likely that the cohesive debris flow deposits (facies **Bmli**)
342 were caused by the activation of water flows associated with lake drainage. The presence of such a
343 sedimentary structure shows continuity in sedimentation at the transition from lacustrine to alluvial
344 deposits. Therefore, no stratigraphic unconformity is present at the base of that facies. Soft-sediment
345 deformation structures are also present in the upper part of the *Cimitero di Atella* succession (Figure
346 9). They consist of boudinage-like breccia structures, made of ash elements in alluvial epiclastic **SBt-**
347 facies sandstone (Figure 8d and Figure 9) and represent a typical case of seismite. Therefore, there
348 must have been synsedimentary seismic activity at that time in the study area (e.g., Pope et al., 1997;
349 Gibert et al., 2011). The above-described facies association can be referred to as a braided alluvial
350 plain with abrupt contributions of primary volcanic products by fallout process and connected to mass
351 deposition by pyroclastic flows.
352 Two fallout ash deposits (lithofacies **Tm**), separated by an eluvial-colluvial horizon (Figure 6), are
353 present at the top of the pyroclastic/epiclastic sequence of the Atella site. Here, a southeast-dipping
354 erosive surface intersects the whole sequence, cutting out a space subsequently filled by historical
355 sediments (Figure 9).

356 4. 2. Dating

357 Atella INF - Ten crystals were individually dated. Nine of them provided a statistically equivalent
358 age within uncertainty, confirming the primary volcanic nature of the deposit. The weighted mean
359 age, calculated using a juvenile crystal population, is 655.2 ± 12 ka (MSWD = 0.2 and P = 1.0, full

external errors at 2σ uncertainties). The $^{40}Ar/^{36}Ar$ initial ratio given by the inverse isochron of 290.8 ± 56 (Table 3) is very unprecise but equivalent within uncertainty to the atmospheric ratio of 298.56 (Lee et al., 2006).

Atella F - Twelve sanidines were individually dated for this layer. The probability diagram obtained for this sample is multimodal and shows a high percentage of reworked volcanic minerals. Only six crystals constitute the homogeneous and youngest population. At least four older eruptive successions are evidenced. The weighted mean age calculated for the youngest population is 577.5 ± 6.4 ka (MSWD = 1.1 et P = 0.3, full external errors at 2σ uncertainties. The $^{40}Ar/^{36}Ar$ initial ratio given by the inverse isochron for this population is 299.4 ± 4.8 (Table 3), equivalent within uncertainty to the atmospheric ratio of 298.56.

Atella I - For this level, unfortunately only six crystals of potassic feldspars were found and successfully dated. Despite the limited number of dated crystals for this layer, these analyses provided significant information. The related probability diagram shows crystals dated from 715 to 575 ka. This crystal age dispersion is very similar to that of level F.

Atella L1 – ESR analyses of this sample provide similar equivalent doses and ages for both Al and Ti-Li centres, indicating good initial bleaching of both signals. A weighted quadratic mean age of 509 ± 56 ka (2σ, full external error, MSWD = 0.051, probability = 0.82) was calculated for this sample using IsoPlot 3.0 software (Ludwig, 2003).

Atella L2 - Thirteen sanidines were individually dated. Again, the related probability diagram is multimodal. Two major crystal populations are evidenced, as well as three older crystals ranging between about 650 and 720 ka (see Figure 10). The younger population included six crystals and gave a weighted mean age of 583 ± 4 ka (full external errors at 2σ uncertainties) (MSWD = 0.9 et P = 0.5 (11 ka). The older crystal population is dated to 610 ± 3 ka. The $^{40}Ar/^{36}Ar$ initial ratio of 297.6 ± 3.0 for the younger population (see Table 3, 2σ analytical uncertainties) is equivalent to the atmospheric one (Table 3).

Atella L3 - Once again, equivalent doses and ages determined from both Al and Ti-Li centres

386 correspond, confirming good initial bleaching of the quartz grains and allowing for the calculation of
387 a weighted quadratic mean age of 442 ± 39 ka (2σ, full external error, MSWD = 0.35, probability =
388 0.55).

389 4.3. Archaeological sequence

390 Our first hypothesis for the archaeological sequence is based on the results of the sedimentological
391 analysis and the first taphonomic observations on faunal and lithic remains. The Borzatti von
392 Löwenstern team initially proposed (Borzatti von Löwenstern et al., 1990) dividing the Cimitero di
393 Atella sequence into 15 geological layers, and two large archaeological units: F and L (Borzatti von
394 Löwenstern et al., 1997). According to Borzatti von Löwenstern, the F level was the result of a
395 lakeshore occupation and level L a redeposition by the river of earlier occupations without handaxes
396 (Borzatti von Löwenstern and Sozzi, 1994; Borzatti von Löwenstern, 2005). Our aim was to re-
397 evaluate site formation and to try to interpret the archaeological records of each level (Figure 11).
398 The combination of an applied excavation method, the study of archaeological finds, and preliminary
399 sedimentological results yields a revised interpretation of the sequence. In the current state of
400 knowledge, we are able to identify four main archaeological units (F-Base, F-Deb2, F-Deb1, L),
401 resulting from different formation processes.

402 At the base of the sequence, we identified F-Base, a first archaeological layer partially excavated
403 by the previous team over about four square metres. This layer is still exposed but was not investigated
404 by us and our interpretation is thus only based on field observations. It contains a high concentration
405 of remains, a *Palaeoloxodon* tusk and other well-preserved macro-faunal remains, and lithic finds
406 consisting of a few handaxes and many small tools and flakes. This horizon lies on top of a palustrine
407 diatomic layer (Figure 11). Human occupation occurred in level F-Base after the retreat of the lake
408 and was covered by a reworked colluvium of fine sediment composed of epiclastic volcanic
409 sandstone, with volcanic angular to sub-angular pebbles (ranging in size from 1 to 10 cm).
410 Preliminary observations on well-preserved remains (fauna and lithic industries), the combined
411 presence of small and large elements, along with the high concentration of finds in fine sediment,

412 indicate that this level is the result of a sub-primary occupation. This hypothesis needs to be confirmed
413 by further analyses after the resumption of excavations in the field.
414 The second archaeological unit (F-Deb2) was extensively excavated by Borzatti von Löwenstern
415 over a surface of 25 m^2 and also by our team over 4 m^2. The material from this level corresponds to
416 the base of level F of the Borzatti von Löwenstern excavation, with a lithic assemblage studied by
417 Abruzzese (et al., 2016). The lithic and faunal remains recorded in this level are in a poor state of
418 preservation. The lithic remains present smoothed edges, often with double patina. The fauna is
419 fragmented and rounded. The concentration of remains is very high in a poorly-sorted matrix-
420 supported epiclastic volcanic breccia, interpreted as a cohesive debris flow deposit. Thus, we
421 postulate that the deposit containing the archaeological record is the result of the reworking of one or
422 several occupations in a secondary position. At this stage, it is difficult to evaluate the degree of
423 reworking of the deposit as well as distance from the primary occupations. Refitting should help to
424 determine whether this corresponds to a major or a light mass movement of the initial occupation.
425 At the top of this reworked deposit, we identified a third archaeological layer covered by the I
426 tephra (F-Deb1). This level was initially called H by Borzatti von Löwenstern and then mixed
427 together with the material from layer F. It was partially excavated by us over a surface of 7 m^2. The
428 thickness of this level varied between a few centimetres to 15 cm, as the top was affected by erosion
429 before being covered by the overlying tephra layer (Figure 8). The lithic and faunal material recorded
430 in this layer is well preserved. The lithic finds present rather fresh edges and no double patina. The
431 assemblage contains a large tool in limestone, small tools and small flakes of different sizes. The
432 faunal remains are less fragmented and rounded and some pieces present fresh surfaces, as for
433 example two Cervidae remains (a coxal and a rib). The archaeological remains are in a fine sediment
434 of epiclastic volcanic sandstone, interpreted as a reworked low-intensity colluvium. The distribution
435 of the archaeological finds, the concentration of material, the presence of small and large pieces and
436 the state of preservation of the remains indicate that the material has not undergone major reworking.
437 We propose that this layer is in a sub-primary position, partially intersected by erosion and quickly

covered by the I tephra layer. Further investigations (use-wear analysis, extension of the excavation, refitting, taphonomic analysis on the fauna, etc) should clarify the degree of coherence of this level.

The last Pleistocene occupations recorded in the site of Atella are in the upper part of the sequence (L). The archaeological finds were found in a coarse epiclastic volcanic sandstone and angular to sub-rounded epiclastic volcanic clast-supported breccia, interpreted as a channel infill by water stream flow of reworked volcanic fallout and pyroclastic flow deposits. This part of the sequence was almost exclusively excavated by the previous team, apart from a small pit in the new area with only a few very small debris found during sieving. The studied lithic material of the Borzatti von Löwenstern assemblage is differentially preserved. Some pieces look very fresh whereas others are smooth and polished. The faunal remains are also differentially preserved. At this stage of the study, this large unit appears to contain material from partially preserved sporadic occupations on a river shore, with differential sorting and erosion depending on the flow of the river.

Thus, based on the results obtained so far, we can identify four moments of occupation at Atella. These layers may be very different in terms of duration, as the F (Deb2) and the L accumulations probably result from several occupations, and it is thus difficult to evaluate their duration. The presence of a palimpsest in secondary position was already known, and we identified at least one well-preserved layer between the F accumulation and the I tephra layer. Given these new and promising data, further investigations at Atella will focus on the excavation of this horizon over a larger surface. Another point to clarify will be the estimation of the time range between occupations, as for the time being, the resolution of absolute dating provides no information concerning the timespan of each unit, nor the period of time between them. Further analyses, especially on the tephra I, should reduce the imprecision of the dating resolution of the sequence.

4. 4. Fauna

The faunal remains are highly fragmented: the most represented size classes are 2 and 3 cm (22.4% and 19.8% of remains respectively) and 81.4% of remains fall within the 1-5-cm interval (Table 6). Most specimens from unit L are unaltered by transport (74%). On the other hand, 38.5% of specimens

464 are rounded (i.e., bone fragments with a spherical or subspherical polished shape) in phase F and
465 43.4% in phase H (Table 7). As most of the faunal remains from Atella are represented by incomplete
466 or fragmented specimens of poor diagnostic value, taxonomic identifications are mainly limited to
467 family or genus, namely ungulates (Bovinae indet., *Cervus elaphus*, *Dama* sp.) or *Palaeoloxodon*
468 *antiquus*/*Palaeoloxodon*-size categories (Table 8). Apart from *P. antiquus*, Borzatti von Löwenstern
469 et al. (1997) reported the presence of a few bovid and cervid remains, and a hyaena tooth. Zucchelli
470 (1999) attributed the Bovinae remains to *Bos primigenius* and Zucchelli (2002) identified *Cervus*
471 *elaphus*, *Dama dama*, and *Capreolus* sp. among the cervids. The revision of the Borzatti von
472 Löwenstern material, in addition to the study of new finds, reveals that some bovid postcranial
473 elements have *Bison*-like features, such as, for example, metapodials (e.g., interarticular incisure U-
474 shaped and less proximally extended in relation to the margin of both condyles; parallel or slightly
475 convergent medial and lateral intercondylar crests). Nonetheless, pending the discovery of new
476 taxonomically significative fossils, the attribution of the bovid material remains opens (Bovinae
477 indet.). No specimens identified so far within the studied sample indicate the presence of hyaenas or
478 *Capreolus* at Atella.

479 4. 5. Palynology

480 Unfortunately, all the analysed levels, excluding those at 6.30, 6.60 and 14.02 m, were barren.
481 After a series of three analysed slides per sample, one *Zelkova* pollen grain was identified in the
482 sample at 6.30 m, one *Pinus* grain at 6.60 m, and one Poaceae grain at 14.02 m, but they were
483 insufficient to define the past vegetation of the site. The lack of pollen grains can be ascribed to factors
484 preventing pollen preservation, the dilution of the pollen content in the sediment due to a very high
485 sedimentation rate, or the occurrence of barren vegetation due to harsh glacial conditions. However,
486 it is also possible that a combination of factors may have contributed to the absence of pollen.

487 4. 6. Lithic industry

488 The analysis of the lithic assemblage confirms the presence of the three main reduction sequences
489 already identified in the Borzatti von Löwenstern assemblage (Abruzzese et al., 2016): small tools,

490 debitage flakes and large tools (Table 5).

491 The first is aimed at small tools confection. This reduction sequence is therefore represented by
492 small tools (266 items, see Table 5) and confection small flakes, namely notch flakes and retouch
493 flakes (268, see Table 5, Figure 12a). The first step consists of blank selection for the future tool. The
494 selected blanks, when determinable, can be small blocks of raw material, flakes, or more rarely
495 residual core fragments. The study of the morphological and volumetric characters of the blank before
496 tool confection brought to light important criteria, such as the small dimensions, the relative thickness,
497 and the presence of a flat surface. Another element can also be present on the initial blank, such as an
498 abrupt surface, for example a back of a *debordant* flake or the butt of the flake. Then, the tool
499 confection phase depends on how the degree of affordance of the blank matches the sought-after tool.
500 This phase consists of shaping and retouching the blank to obtain several cutting edges. The removals
501 generally come from the flat surface of the blank and concern the transformative part of the future
502 tool and in some cases the prehensile part. On the cutting edges, several modalities of confection are
503 performed from short, low and parallel removals to notched abrupt retouch. The management of the
504 prehensile part is rarer and consists mainly of the correction or accentuation of an abrupt part.
505 Consequently, the flakes from the confection of these small tools are varied and depend on the features
506 of the initial blank and of the sought-after tool. Notch flakes are short and wide and characterized by
507 a thick and convex butt (Figure 12a). Retouch flakes are thin and curved, with a linear or punctiform
508 butt, and the dorsal surface can present previous retouch scars.

509 The aim of this reduction sequence is to obtain several cutting-edges on small tools. The tool
510 sample is too small for the moment to describe this techno-functional group in detail. It consists
511 mainly of rostrums, trihedral, and rectilinear edges, as observed in the previous publication
512 (Abruzzese et al., 2016). The illustrated example (Figure 13) presents three transformative parts
513 (TFU1, TFU2, TFU3) on the same piece, each associated with a prehensile part. The transformative
514 part consists of a trihedron composed of a flat surface, two facets obtained by lateral notches, and a
515 central ridge (Figure 14). Only part of the whole volume is modified to fashion the tool. The

prehensile part, in this case a prepared back, can be adapted to several transformative parts. From a production point of view, several gestures and probably several hammerstones were used to make this small tool. For the management of convexities and the production of the flake, blows are internal, probably made with a hard hammer. The back is obtained by an orthogonal gesture (fracture blow). The notches blow, important to highlight the trihedrons are internal and were probably made with a smaller hammerstone.

The second reduction sequence consists of flake production. Due to the rarity of whole cores in the assemblage (25 items, mainly fragments, Table 5), it is difficult at this stage of the study to define flaking modes and the objectives of flake production based on core analysis. The few cores belong to an additional production system (Boëda, 2013; De Weyer et al., 2022). The exploited volume of the cores only represents a small part of the initial blank. No cores show global preparation of volume, or partial management of convexities. The flaking sequence is very short, with no more than five removals per core. Flake scars indicate the production of elongated and quadrangular flakes, with large butts, two cutting edges or one cutting edge and a back. The entire core and fragments are in flint and quartzite. This scant information from the cores is consistent with data from flakes. The latter (401 items, Table 5) are elongated or quadrangular, with one or two scars on the dorsal surface and often present a natural back (Figure 12b). These large flakes in flint and quartzite are never retouched, but present one or two cutting edges. The characteristics of these flakes, dimensions and technical features are different from the small flakes issued from making small tools. This category of large flakes is compatible with core attributes, indicating that they are flakes from the debitage reduction sequence. Some of these flakes may have been used as blanks for small tools, but as the latter are highly reduced, it is difficult to identify the initial blank. The debitage reduction sequence can also be interpreted as a goal in itself, to obtain a longer cutting edge. This component is almost always present in Lower Palaeolithic assemblages. Further investigation into this debitage reduction sequence and the relationship between small tools and flakes is required in the future, on a larger sample, particularly of cores.

The large shaped tools constitute the third reduction sequence. This category comprises what we can call, from a typological point of view, Large Cutting Tools, handaxes, unifacial pieces, and pebble tools (28 items, Table 5). These tools are mainly made on poorly-preserved limestone pebbles and analysis is therefore difficult. From a production point of view, the chosen blank is plano-convex, and can be a pebble or a large cortical flake. Shaping is mainly limited to the upper apical part of the blank, and the basal part is unretouched. The shaping phase takes into account the volumetric characteristics of the chosen blank and only affects the future transformative part, as the prehensile part is rarely modified. This very short shaping phase does not affect the volumetric structure of the blank. We were not able to identify flakes from this reduction sequence. This is maybe due to the poor state of preservation of the limestone, particularly affecting on thin and small shaping flakes. It is also important to recall that macro-tools are very rare in the assemblage and bear a low number of scars. The technical features of large tools show that shaping flakes may present a cortical, semi-cortical surface or positive scar on the dorsal surface. Due to shaping modes, the classical expected features for shaping flakes, such as a curved profile, an open angle between the ventral surface and the butt, and soft hammer percussion, may not be determinant here. Indeed, flakes from large tool shaping do not bear specific features, and it is thus difficult to distinguish them from other flakes.

The identification of this techno-functional group is problematic due to the low number of large tools. At this stage of the analysis, the main categories of large tools are represented by distal rostrums and in one case by a lateral cutting edge (Figure 15).

Thus, the assemblage of Cimitero di Atella studied so far is composed of three main reduction sequences. The main one, in term of the number of items and techno-functional variability, is represented by the small tools. Large shaped tools and backed flakes are less frequent and for the moment, we can go no further with our interpretation due to the limited quantity of elements.

5. Discussion

5. 1. Site of Atella

5.1.1 Geology

As a result of field investigations, following the stratigraphic framework proposed by Giannandrea et al. (2006) and Schiattarella et al. (2016), we correlated the basal 1-m-thick portion of lacustrine sediments (facies Sh in Figure 6) with the Rionero Subsystem and, consequently, we were able to correlate the overlying volcanic (facies **Tm**, **Tng**, **LTm**, and **TLm**) and lacustrine layers, up to the epiclastic layers of the facies **Bmli** (unit F of Borzatti von Löwenstern et al., 1997), with the Vulture - San Michele Subsynthem. The presence of soft-sediment deformation structures in lacustrine sediments below the **Bmli** facies suggests that the deposition of unit F of Borzatti von Löwenstern (et al, 1997) occurred immediately after the lake was drained, when the fine sediments were still saturated. It is also likely that the cohesive debris flows (facies **Bmli**) were deposited by the activation of water flows associated with lake drainage. This sedimentary structure shows continuity in sedimentation at the transition from lacustrine to alluvial deposits. Therefore, no stratigraphic unconformity is present at the base of the archaeological fluvial facies. Also, sedimentological analyses performed in unit L of Borzatti von Löwenstern (et al., 1997) reveal tephra layer intercalations, interpreted as pyroclastic flow, in the fluvial facies. Considering the presence of seismically-induced soft-sediment deformation structures, this can be ascribed to particularly intense and voluminous eruptions of the Monte Vulture volcano.

5.1.2 Geochronological interpretations

Based on the geology, archaeology, and palaeontology of the site, Borzatti von Löwenstern et al. (1997) proposed a date for the Cimitero di Atella sequence between about 600 and 500 ka. Later, Di Muro (1999) suggested correlating stratigraphic levels A to E with the Rionero Subsynthem of Monte Vulture (i.e., 630 ± 20 ka to 714 ± 18 ka following Villa and Buettner, 2009). While our new individual data obtained by $^{40}Ar/^{39}Ar$ and ESR on bleached quartz appear insufficient for accurately determining the ages of the Cimitero di Atella archaeosurfaces, combining this new geochronological dataset with

591 the available geological information helps to constrain the period of human occupations with greater
592 confidence and accuracy.

593 Concerning the $^{40}Ar/^{39}Ar$ analyses, the lowest level dated by this technique, Atella INF (Tng
594 primary volcanic layer, see Table 3, Figure 10) is accurately dated to 655 ± 12 ka, the maximum age
595 for the entire sequence of the Cimitero di Atella archaeological site. The analytical data for levels F,
596 I, and L2 are more difficult to interpret, as all the corresponding probability diagrams are complex
597 and multimodal (see Figure 10), suggesting the massive reworking of volcanic materials from several
598 eruptive events, the youngest of which is dated to around 570-580 ka. The various ages of the oldest
599 populations of crystals can be attributed to the first part of the Monte Vulture volcano eruptive activity
600 (between about 610 and 760 ka), corresponding to the San Michele and Rionero Subsynthem
601 activities (Villa and Buettner, 2009). For these three dated stratigraphic levels, the youngest sanidines
602 are all dated to around 580-570 ka. This age can only be considered here as a maximum age for the
603 deposition of the Cimitero di Atella archaeological horizons. It is noteworthy that even if the Monte
604 Vulture volcano was very active from the beginning of the Middle Pleistocene until 490 ka, it was
605 nonetheless characterized by a long phase of quiescence between about 570 and at least 530 ka,
606 followed by an eruptive sequence after local tectonic activity (i.e., Case Lopes subsynthem).
607 Therefore, the fact that no eruptions more recent than about 580-570 ka were recorded in levels F, I,
608 and L2, can be taken as a further chronological indicator. Deposits from the Case Lopes Subsynthem
609 are dated to 530 ± 22 ka and 494 ± 5 ka (Villa and Buettner, 2009, Monticchio Supersynthem) and
610 found a few kilometres NE of the site but not found in the reworked and dated volcanic material at
611 Cimitero di Atella. Even though the absence of such deposits cannot be considered as chronological
612 proof of the antiquity of the archaeological remains, it nevertheless implies that the Cimitero di Atella
613 sequence predates the Case Lopes eruptive phase. This hypothesis is reinforced by the ESR ages
614 calculated for L1 (509 ± 46 ka) whereas L3 (442 ± 39 ka) suggests a younger age for the deposition
615 of the upper part of the sequence. Even if these ages lack precision, they provide a needed
616 chronological framework for the deposition age of the sedimentary sequence of Cimitero di Atella.

They also demonstrate the continuity of the stratigraphic sequence and reinforce interpretations based on the geology and $^{40}Ar/^{39}Ar$ data. They allow us to determine a deposition age between L1 and L3 (509 ± 46 ka - 442 ± 39 ka). The age of 509 ± 46 ka also provides a minimum age for the archaeological levels underlying L1 (F unit). The combined geochronological data therefore suggest that at least the lower Palaeolithic F levels can be securely dated between 509 ± 46 ka and 570-580 ka, covering the end of MIS 15 until MIS 13 (Figure 10).

5.1.3 Palaeobotany

Previous pollen analyses at Cimitero di Atella were carried out on 15 pollen samples by Borzatti von Löwenstern von Löwenstern et al. (1998). However only four levels presented enough pollen grains to describe the surrounding environment, namely levels A01, A02, A03 and I. According to the new chronology of the Borzatti von Löwenstern sequence presented here, these levels were deposited between 655 ± 12 and 575 ± 7 ka BP. The pollen content of A02, A03, and I, showing Arboreal Pollen (AP) percentages above 88%, *Abies* up to 15%, *Quercus* deciduous ranging from 7 to 35%, and many other deciduous and evergreen broadleaved trees in low frequencies, suggests a cool and wet phase of the interglacial stage corresponding to MIS 15. Conversely, in the underlying level A01, the AP percentage (76%) with 53% *Pinus*, and high proportions of bush and herbaceous xeric taxa, such as *Ephedra*, *Artemisia*, and Poaceae, suggest an arid phase during the MIS 16 glacial stage.

5.1.4 Occupation modes

In the current state of knowledge, it is difficult to accurately reconstruct the human occupations of Cimitero di Atella. However, some new data contribute to a better understanding of the type of occupation. Overall, the stratigraphic succession registered several episodes of human presence between 0.58 and 0.44 Ma. At that time, the landscape changed from a lacustrine to a fluvial environment in a territory highly impacted by the activity of Monte Vulture. The recording of human occupations is different in term of temporality. Some layers, such as F-Deb2, are probably a mix of several occupations, of unknown duration, whereas others, like F-Base and F-Deb1, probably result from a single “moment” of occupation, including tool making and faunal exploitation. The future excavation of unit L, corresponding to the fluviatile sequence, will provide crucial information. The

archaeological record shows that such contexts are propitious to simultaneous faunal and human occupation and to the quick burial of their tracks. Unit L, as already observed by Borzatti von Löwenstern (2005, 2011), could contain several more or less well-preserved occupation "spots", depending on site formation taphonomy (velocity of sedimentation, the riverbed position and flow intensity). The presence of rich but mixed units alongside short well-preserved occupations in the sequence is interesting and is in our opinion complementary. The secondary position (colluvium) of the unit is not conducive to spatial or techno-economic analysis, but the material is useful for a more global view of technical variability. Conversely, the level interpreted as an occupation surface may contain important information on occupation modes, spatial organization, faunal exploitation and tool manufacture and use. At Atella, given the type of sedimentation, we are probably not in presence of a genuine snapshot, as observed at Ficoncella (Aureli et al., 2015; Boschin et al., 2018), Soucy 3 (Lhomme, 2007), La Polledrara di Cecanibbio (Santucci et al., 2016), and Schöningen (Serangeli et al., 2015), but rather a sub-primary position site resulting from one or more occupations in a relatively short time period, like in some levels of Notarchirico (Piperno et al., 1999) and Isernia La Pineta (Peretto et al., 2004). It is interesting to note that in both levels (F-Base and F-Deb1), like in other many contemporaneous sites, human occupation is linked to an aquatic environment (lake and river) with large herbivores, especially elephants (Kodinaris et al., 2016; Rocca et al., 2021). The relationship between humans and elephants also needs to be reassessed, beyond the hunting/scavenging debate, in order to really focus on exploitation modes and purposes. For meat? For toolmaking or other technical activities? What was the impact of the elephant on the landscape? Was the carcass a landmark in the territory? etc. We hope that the extension of the excavation surface to about 250 m^2 will reveal new information on site formation and spatial organization, in order to enhance our interpretations of occupations at Atella.

5.2. Atella in a broader context

5.2.1. Is it relevant to speak about an Early Acheulean?

The south European Lower Palaeolithic panorama has been extensively reshaped in recent years.

Until the end of the 1990s, this cultural period was divided into two lengthy phases on the basis of typological studies; an older one, called the pre-Acheulean without handaxes, and a younger one, including Acheulean, Clactonian and Tayacian industries (Palma di Cesnola, 2001; Grifoni and Tozzi, 2006). New data, mainly from the sites of Isernia La Pineta and Notarchirico, call into question this model. At the end of the 1990s, new dates from Notarchirico significantly pushed back the age of early handaxes in Europe (Pilleyre et al., 1999; Piperno et al., 1999). Then, conversely, in the 2010s, the new dating of Isernia La Pineta, a site without handaxes, attributed the site to a more recent period (Peretto et al., 2015). Those new data led to a reconsideration of the Lower Palaeolithic periodisation, alongside the development of lithic industry study methods. The Isernia La Pineta team applied new methods, such as technology, experimentation, use-wear analysis, resulting in the criticism of Tayacian typology (Crovetto, 1993; Crovetto et al., 1994; Peretto et al., 1994; Longo et al., 1997). The discovery of new early sites with handaxes in Europe in the 2010s led to the construction of a new chrono-cultural model (Moncel et al., 2013, Garcia-Medrano et al., 2014, Mosquera et al., 2016). These early occupations (Arzarello et al., 2012; Ollé et al., 2013; Michel et al., 2017; Despriée et al., 2018) brought to light a new conception of tools in Europe from about 0.8/0.7 Ma, based on the handaxe or Large Cutting-Tool, called the Early Acheulean (Moncel et al., 2015, 2020; Moncel and Schreve, 2016). Thus paradoxically, after a short parenthesis focusing on the reduction sequence and technical diversity, we are now returning to a very typological definition based on the Acheulean guiding fossil: the biface. Indeed, the origins of the Early Acheulean in Europe are often implicitly and schematically explained using the following model:

Presence of a phase of core and flake industries between 1.4 Ma and 0.8 Ma (Mode 1) and the arrival from Africa of new industries with handaxes (Mode 2), from 0.8/0.7 Ma onwards, spreading rapidly to the north (La Noira) and south (Notarchirico, la Boella) of the European continent. Can we really define this period on the basis of a single tool? What can other ways of making tools, such as flake production or the so-called small tools tell us? Do we have solid proof of an external arrival of this new technical tradition? Is it relevant for researchers to coin the term Early Acheulean in studies of

696 this key period of the Palaeolithic? How can the lithic industries of Cimitero di Atella contribute to
697 an enhanced definition of this period?

698 The assemblage of Cimitero di Atella studied so far is consistent with the other contemporaneous
699 technical system, the so-called Early Acheulean. As in other sites, abundant small tools and/or flakes
700 play an important role in tool kit variability, while large shaped tools are rare (Nicoud et al., 2016;
701 Tourloukis et al., 2018; Grimaldi et al., 2020). Furthermore, large tools are significantly different to
702 the Acheulean handaxes that emerge in the second part of the Lower Palaeolithic, in that shaping does
703 not affect the global volume of the blank and is aimed at obtaining a specific cutting edge, mainly
704 rostrums. Edge-point bifacial tools are very rare, as well as lateral cutting edges. At Atella, as
705 elsewhere, these shaped tools display wide technical diversity: each specimen is almost a specific
706 tool type. This diversity is also present for example at Notarchirico (Moncel et al., 2019, 2020; Nicoud
707 2011), and at la Boella (Mosquera et al., 2016).

708 Further discussion is required to enhance our understanding of the specificity of this ambiguous
709 category of large tools in the Early Acheulean. Nicoud (2011) proposes the term “pebble with bifacial
710 removals”, as does Moncel (2019, 2020), to distinguish “bifaces and bifacial tools” from “pebble
711 tools” at Notarchirico. Mosquera (et al., 2016) groups together all the shaped pieces under the term
712 “large cutting-tools”. A more in-depth investigation of this category of tools is now required, focusing
713 on techno-functional aspects. Paradoxically, early large cutting-tools are overrepresented in
714 publications, despite their small numbers, but are rarely studied in relation with other
715 contemporaneous tools and compared with younger handaxes. We choose to call these pieces from
716 Atella large shaped tools, because they cannot all be considered to be bifacially shaped from a
717 technological point of view. Yet it would be illogical to distinguish bifacial from non-bifacial large
718 tools, as they can present the same morpho-technical features. However, we can note that these pieces
719 are different from classical handaxes in terms of volumetric structure and techno-functional features.
720 Even more surprisingly, some transformative parts, such as the rostrum, for example, seem to be
721 comparable to ones on small tools in terms of technical-functional features and techno-productional

modes. In terms of weight and dimensions, use, but also probably prehension modes, these tools are clearly distinguishable from their smaller counterparts. But it is nonetheless interesting to approach the relationships between several categories without always considering these first handaxes as an archaic model of future Acheulean bifacial pieces.

The small tool category also necessitates further discussion. The presence of small tools was recognized in Tayacian typology (Tayac and Quinson point), but the variability and importance of this category was subsequently re-evaluated in Central European and Middle Eastern assemblages (Burdukiewic and Ronen, 2003). In line with this work, we attempted to better define this part of the lithic assemblage from a technological and techno-functional point of view (Aureli et al., 2016; Rocca 2016; Rocca et al., 2016). The term small tool can be misleading, since it emphasizes size, rather than the technical reality of this specific reduction sequence. Indeed, the presence of small and thick tools on specific selected blanks with a flat surface opposed to a convex surface, with cutting edges, is widespread. Regardless of the term, this specific tool kit is a crucial element for characterizing the technical system of this phase of Lower Palaeolithic.

In sum, the results obtained on the lithic assemblage of Cimitero di Atella contribute to a better knowledge of the technical system in Southern Europe. The tool kit is mainly obtained by the confection of small tools and secondarily by shaping large tools and flaking backed flakes. Many questions still need to be addressed in the future, including the selection/production of blanks and the techno-functional diversity of small and large tools. But in our opinion, in order to better comprehend this phase of the Lower Palaeolithic, we need to examine the whole assemblage, not only LCTs, from a technological perspective.

5.2.2. *The fauna of Atella in a broader context*

The Early Acheulean spread throughout Europe alongside considerable faunal turnover, in a broader context of remarkable environmental and climatic changes. Consequently, the period between the latest Early and Early Middle Pleistocene (~1.2-0.5 Ma) is often referred to as the Mid-Pleistocene Revolution, or Early–Middle Pleistocene Transition (EMPT). The EMPT witnessed a climatic change

748 of paramount importance: the increase in the amplitude of glacial-interglacial oscillations, a shift that
749 in turn prompted sharper recurrent changes in associated phenomena, such as, for instance, ice volume
750 cycles (Clark et al., 2006; Head and Gibbard, 2015; Maslin and Brierley, 2015). The mutated (and
751 more instable, at a ~100 kyr temporal scale) climate conditions favoured the spread of adaptable
752 species, which eventually completely replaced previous Villafranchian mammals by the end of the
753 EMPT (Gliozzi et al., 1997). These animals include several forms closely related to extant lineages
754 or species, for instance, red deer, wild boars, hyenas, and wolves (van der Made et al., 2017; Iannucci
755 et al., 2021a; Iurino et al., 2022). The general pattern is quite clear, but these bioevents did not all
756 occur at once, as the different species reacted variously to environmental changes. As emphasised by
757 several authors (Martinez-Navarro et al., 2010), investigating the faunal response and the timing of
758 bioevents can provide relevant clues on potential coincidental diffusions of hominin populations or
759 lithic tradition.

760 The faunal list of Atella should still be considered to be provisional, as the ongoing excavations
761 will yield new material that will contribute to refining current attributions and possibly identify new
762 species. However, some considerations can be noted. The straight-tusked elephant, *Palaeoloxodon*
763 *antiquus*, is the best-represented species at Atella. An isolated molar recovered from the latest Early
764 Pleistocene of Slivia, in north-eastern Italy (~0.9–0.8 Ma) is the earliest record of this elephant in
765 Europe (Bon et al., 1992), which becomes much more abundant during the Middle Pleistocene
766 (Palombo and Ferretti, 2005). In Italy, the latest well-dated occurrences of the species are not recorded
767 after MIS 5 (Braun and Palombo, 2021; Mecozzi et al., 2021b; Pieruccini et al., 2022). The straight-
768 tusked elephant is more frequently reported during interglacial stages, but the species was a mixed
769 feeder and inhabited different environments (Palombo et al., 2005; Rivals et al., 2012).

770 The red deer, *Cervus elaphus*, is also documented in some latest Early Pleistocene localities,
771 including Atapuerca, Dorn-Dürkheim, and Slivia (Bon et al., 1992; Franzen et al., 2000; van der Made
772 et al., 2017), while it becomes widespread in Middle Pleistocene assemblages (Di Stefano et al., 2015;
773 van der Made et al., 2017). Again, *C. elaphus* is an adaptable species with a wide ecological tolerance

774 and flexible feeding behaviour (Gebert and Verheyden-Tixier, 2001; Benvenuti et al., 2017).

775 Few remains attest to the presence of the fallow deer, *Dama* sp., at Atella. The taxonomy of *Dama*-
776 like deer is far from unanimously agreed upon (e.g., Di Stefano and Petronio, 2002; Breda and Lister,
777 2013; van der Made et al., 2017; Croitor, 2018), and thus it is somewhat contentious to attempt to
778 place occurrences of the genus in a chronological context. Differences in Middle Pleistocene fallow
779 deer are mainly documented on antlers, and when these are not available, specific attributions are
780 often based on chronological grounds. In any case, fallow deer are common during the Middle
781 Pleistocene, but are usually reported in localities related to interglacial stages (Mecozzi et al., 2021c).
782 Moreover, although the diet of extant fallow deer populations varies in many respects (Esattore et al.,
783 2022), a browsing behaviour is generally inferred for Middle Pleistocene fallow deer (Rivals and
784 Ziegler, 2018; Strani et al., 2022).

785 The Atella bovids cannot be confidently identified at a species level (*contra* Zucchelli, 1999), even
786 though some bones show *Bison*-like features. Nonetheless, this group arouses much interest within
787 the context of Acheulean diffusion in Europe, with Martínez-Navarro et al. (2010) emphasising a
788 coincidental spread of the Acheulean culture and *Bos*. This was supported in particular by the
789 attributions of the material of Notarchirico and Loreto to *B. primigenius* (Caloi and Palombo, 1979;
790 Cassoli et al., 1999). However, subsequent research has pushed back the chronology of Early
791 Acheulean diffusion into Europe (see section 5.2.1.), while the taxonomic identification of the scant
792 postcranial bovid material recovered from the aforementioned localities of the Venosa Basin requires
793 further investigation (Iannucci et al., 2021b). Incontestable *B. primigenius* cranial remains are only
794 documented since ~0.5 Ma. As in the case of the other species, the representativeness of *B.*
795 *primigenius* in the fossil record increased at a later stage, during the late Middle to Late Pleistocene
796 (Wright, 2013; Iannucci et al., 2021b).

797 To sum up, the species encountered at Atella represent a typical assemblage for the Middle
798 Pleistocene of Italy. Most of them are characterized by high ecological tolerance, but some indications
799 (abundance of *P. antiquus*, presence of *Dama* sp., absence of species mainly related to cold and open

800 habitats) suggest a warm, perhaps interglacial, environment.

801 *5.2.3. Environmental evolution*

802 In Central and Southern Italy, the 650-500 cal. BP time interval, encompassing the site of Cimitero
803 di Atella, is characterized by major vegetation turnover, revealed by a number of pollen records
804 spanning at least part of this interval, stretching from MIS 16 to the first part of MIS 13.

805 MIS 16 is recorded at Vallo di Diano, the largest tectonic basin of the Southern Apennines, located in
806 the Campania region, ca. 50 km south of Cimitero di Atella (Russo Ermolli, 1994; Russo Ermolli and
807 Cheddadi, 1997). The pollen record reveals a semi-open landscape with steppe vegetation dominated
808 by Poaceae, *Artemisia* and other Asteraceae species. Conifers were mostly represented by *Pinus* and
809 *Abies*, especially at the transition with MIS 15, when steppe taxa declined. Apart from oaks,
810 broadleaved trees were represented by scattered occurrences. The contents of pollen sample A01 in
811 the Borzatti von Löwenstern sequence match the final part of MIS 16 at Vallo di Diano.

812 MIS15 is recorded at Vallo di Diano and in the Sessano Basin (Russo Ermolli et al., 2010), a large
813 tectonic depression located in Molise. The pollen record of this interglacial period points to a
814 remarkable development of broadleaved woodlands dominated by deciduous oaks with *Ulmus*,
815 *Zelkova*, *Carpinus*, and *Acer*, accompanied by sparse evergreen formations composed of evergreen
816 oaks and Ericaceae. The permanence of conifers in the landscape is revealed by significant
817 frequencies of *Abies*, suggesting cool and wet conditions, and *Pinus*. Some steppe vegetation was
818 also present in this environment, despite increased humidity. Overall, the vegetation features
819 documented by samples A02, A03 and I of the Borzatti von Löwenstern sequence are similar to some
820 MIS15 pollen spectra from Vallo di Diano. A remarkable ecological and biostratigraphic aspect of the
821 Borzatti von Löwenstern sequence is the occurrence of *Tsuga* (<3%) in samples A01 and A02. In
822 Central Italy, the last significant abundance (>5%) of this conifer occurs in the Torre Mucchia record,
823 correlated with MIS 17 (Pieruccini et al., 2016; Magri et al., 2017). It probably persisted until MIS
824 13, when it occurred at Sessano (Russo Ermolli et al., 2010). Thus, the presence of *Tsuga* at Atella is
825 consistent with the new chronology of the site and shows that sparse populations of this tree were still

826 present in the Italian Peninsula during the Middle Pleistocene.

827 MIS 14 is well represented in the pollen records of Vallo di Diano, Sessano, and Acerno. The latter
828 site is a narrow tectonic depression located in the central sector of the Picentini Mts, ca 50 km west
829 of Cimitero di Atella (Munno et al., 2001). The vegetation history of this period points to a new
830 decline of forests, in particular broadleaved trees and shrubs, alongside a marked expansion of steppe
831 vegetation, but with clear floristic differences in the three sites. At Vallo di Diano, a progressive
832 decline in deciduous oaks is coeval with an abrupt conifer turnover, with a clear reduction of *Abies*
833 and a new expansion of *Pinus*. At Sessano, deciduous oaks declined more markedly, accompanied by
834 the disappearance of almost all the broadleaved trees and *Abies*. At Acerno, broadleaved trees were
835 still abundant, at some point with *Betula*. In general, climate conditions during glacial phases MIS 16
836 and MIS 14 do not seem sufficiently harsh to wipe out temperate forests, and plants and animals may
837 have persisted for some time in glacial refuges in Southern Italy (Orain et al., 2013).

838 The vegetation history of the MIS 13 interglacial phase has been reconstructed from several sites in
839 Central and Southern Italy, including (from north to south) Rignano Flaminio (Di Rita and Sottili,
840 2019) and Ceprano from Lazio (Margari et al., 2018), Sessano (Russo Ermolli et al., 2010) and Boiano
841 from Molise (Orain et al., 2015), Acerno (Munno et al., 2001) and Vallo di Diano (Russo Ermolli et
842 al., 1994, Petrosino et al., 2014a) from Campania, and the Mercure Basin at the Calabria-Basilicata
843 boundary (Petrosino et al., 2014b). These sequences suggest that local environmental factors
844 (including edaphic, topographic and climatic conditions) led to the development of specific forest
845 landscape characters in each site, which are difficult to place in regional vegetation patterns (Russo
846 Ermolli et al., 2015). In the pollen records closest to Cimitero di Atella, namely Vallo di Diano and
847 Acerno, forests were dominated by deciduous *Quercus* and *Abies*, with a still conspicuous presence
848 of *Pinus*. It is likely that these trees were also the main floristic elements of the woodlands
849 surrounding Atella during MIS 13.

850 6. Conclusion

851 The new stratigraphic, sedimentological and geochronological data identified tephra layers in the

852 sediments of the Cimitero di Atella archaeological site, interpreted as fallout deposits and pyroclastic
853 flows related to the eruptive activity of the upper portion of the Monte Vulture Supersynthem (starting
854 at the boundary between the Rionero and Vulture-San Michele subsynthems). $^{40}Ar/^{39}Ar$ dating on the
855 lowest tephra layer (Atella INF) of the measured stratigraphic section dated the base of the Vulture –
856 San Michele Subsynthem to 655 ± 12 ka. Sedimentological analysis also correlates the **Bmli** and **Suli**
857 facies (archaeological unit F of Borzatti von Löwenstern et al., 1997) with the draining of the lake.
858 According to our $^{40}Ar/^{39}Ar$ dating of the F horizon of Atella, this dramatic event should have taken
859 place at about 570-580 ka. The erosional surface at the top of these sediments indicates a
860 morphological development of an alluvial channel, subsequently filled by 2.5-m-thick volcaniclastic
861 braided-type alluvial facies with intercalations of primary volcanic layers. These sedimentological
862 data suggest a volcanic reactivation of Monte Vulture Volcano, leading to an increase in the
863 sedimentary load in an alluvial environment. The presence of seismically-induced soft-sediment
864 deformation structures can be related to eruptions with sufficient energy to quake the Atella territory.
865 Geochronological analyses carried out in the alluvial part of the stratigraphic section suggest
866 sedimentation between 509 ± 46 ka and 570-580 ka. These data do not allow us to accurately identify
867 the upper limit of the Vulture - San Michele Subsynthem nor to link the deposits from the upper
868 portion of the Cimitero di Atella section to the younger eruptive stages of the Monte Vulture
869 Supersynthem. Therefore, in order to date the archaeological site more accurately, and also in relation
870 to the stratigraphic scheme of Monte Vulture Volcano by Giannandrea et al. (2006), in the future we
871 aim to collect further sedimentological, geochemical, and geochronological data from the portion
872 revealed by ongoing excavations of the site and to perform stratigraphic checks in the Monte Vulture
873 volcanic sequence.

874 Archaeological investigations identify at least four occupation episodes at the site during the
875 second phase of the Lower Palaeolithic. They are different in terms of preservation and probably
876 accumulation duration, but these occupations belong to the same techno-cultural context, and are
877 consistent with other more or less contemporaneous sites in Italy and Western Europe. The tool kit is

obtained in three main ways: small tool confection, flake debitage and LCT shaping. The specific productional and functional attributes of these categories need to be clearly defined in the future, along with discussions of the definition of these typical Early Acheulean productions. The still preliminary results from the techno-functional analysis of small tools reveal the technical complexity of this phase of the Lower Palaeolithic. The nature of interactions between human groups and fauna will also be developed, in particular after the extensive excavation of level F-Deb1, the most promising in terms of preservation and deposition duration. The faunal elements identified so far constitute a typical assemblage for the Middle Pleistocene of Italy, with abundant straight-tusked elephants *Palaeoloxodon antiquus*, bovids and cervids. *Palaeoloxodon antiquus* and fallow deer *Dama* sp. are more frequently recorded during interglacial stages, and Middle Pleistocene fallow deer are usually associated with a browsing feeding behaviour. The identification of an elephant footprint at the top of tephra I by Borzatti von Löwenstern will need to be confirmed by fieldwork. Last year, new work focused on the ichnological sources, of animals but also humans (Altamura et al., 2020; Duveau et al., 2019; Mayoral et al., 2021). The development of this approach, based on more samples and new technical methods, will also reconsider the Atella trace found in the 1990s and explicitly look for other possible footprints. The study of the fauna will focus on faunal procurement but also on carcass exploitation for alimentary or technical purposes, as in other contemporaneous contexts (Boschian and Sacca, 2015; van Kolfschoten et al., 2016; Tourkoulis et al., 2018; Aranguren et al., 2019; Villa et al., 2021). Future investigations at Atella, in the field and on the material will assess the degree of preservation of each occupation and better define the technical system. Then these results need to be compared with results from other sites in Italy and in Europe also under study, and placed in a broader context.

Acknowledgment:

We would like to thank the institutions that support the Atella project. The Soprintendenza Archeologia Belle Arti e Paesaggio della Basilicata, the French school of Rome, the Basilicata region and the municipal administration of Atella.

Table:

Table 1: Description of Monte Vulture Volcano stratigraphic units (after Giannandrea et al., 2004, 2006; Stoppa et al., 2008). Unit codes correspond to those of the official 1:50,000-scale geological sheet (Foglio 451 Melfi, Carta Geologica d'Italia, 2010).

Table 2: List of pyroclastic and epiclastic lithofacies with brief descriptions and interpretations

Table 3: ESR data and ages obtained for Atella samples.

Table 4: Number of archaeological finds

Table 5: Distribution of lithic artefacts by technological category. Retouch flakes: small retouch flakes, notch flakes, small flakes of from the confection of small tools; Small tools: entire and fragmented small tools; Cores: entire cores and core fragments; Flakes: production flakes from a flaking reduction sequence; Large tools: Handaxes and large shaped tools; Indet: debris, indeterminate small fragments, chunks

Table 6: Size of faunal specimens in the whole site

Table 7: Alteration of fragments

Table 8: Taxonomy of faunal remains according to stratigraphy

Figures:

Figure 1: Map of the region. A. Atella and Venosa Basin in Southern Italy; B. Picture of the Atella Basin (archivio scavo Borzatti von Löwenstern).

Figure 2: a. Geological sketch map of Southern Italy; b. DEM-based sketch map of Monte Vulture volcano and Atella and Venosa mid-Pleistocene basins, with location of the Cimitero di Atella site.

Figure 3: a. Detailed geological map of the Atella area; b. geological cross-section through the Cimitero di Atella site.

Figure 4: (a), position of the cores (b) Cimitero di Atella excavation plan with the location of the different excavation areas from 1990 to 2021.

Figure 5: Panoramic view of the study area with Monte Vulture volcano in the background showing the Atella sub-horizontal landsurface.

Figure 6: Sedimentary log with indications of lithofacies and facies associations, correlation with previously published units (Borzatti von Löwenstern et al., 1997; Giannandrea et al., 2006), and 40Ar/39Ar and ESR dating samples.

Figure 7: Photos showing some Cimitero di Atella site lithofacies: a) thinly laminated epiclastic volcanic siltstone, Sh; b) fine- to coarse-grained massive tuff, TLm (black triangles indicate co-current falls); c) fine- to medium-grained normal graded tuff, Tng; d) three beds made of fine-grained structureless (the lowermost bed) and poorly laminated (the upper two beds) tuff, Tm; e) epiclastic volcanic breccia (lithofacies Bmli) sandwiched abruptly between two reworked colluvium deposits, Suli (black triangles indicate the basal erosive surface; white triangles indicate the upper boundary of the Bmli bed consisting of an articulated erosive surface); at the top, a tusk of Palaeoloxodon antiquus unconformably covers the Bmli and Suli lithofacies. Details of lithofacies codes in Table 2.

Figure 8: Photos showing some lithofacies from the upper part of the Cimitero di Atella site: a) fine-grained lacustrine beds of lithofacies Sh, Dh, and Su, under the lithofacies Bmli, coarse-grained deposits (triangles indicate soft-sediment deformation structures: black triangle indicates dome-like flame structure, and yellow triangle indicates simple load casts); b) alluvial fine (Sr)- to coarse (SBt)-grained epiclastic sandstone abruptly overlain by a massive pyroclastic deposit of lithofacies LTm; c) pyroclastic bed of lithofacies TLBm, showing at the base dome-like flame structure (white triangles); d) from the bottom: bed of pyroclastic deposit of lithofacies TLm, sandwiched between alluvial sediments made of a mixture of pyroclastic (Lm) and epiclastic (SBt) lithofacies (yellow triangles indicate simple load cast structures; white triangles indicate the erosive surface at the top of the lithofacies Lm; black triangles indicate the depositional surface of the lithofacies Lm above the alluvial sediment SBt); in the upper portion, irregular ball-and-pillow morphology (red triangles indicate boudinage-like breccia structures). Details of lithofacies codes in Table 2.

Figure 9: Depositional architecture of alluvial facies association outcropping in the upper portion of the Cimitero di Atella succession (yellow triangles indicate load structures; red triangles indicate irregular ball-and-pillow structures); lithofacies codes reported in Table 2.

Figure 10: $^{40}Ar/^{39}Ar$ and ESR results obtained on Atella samples, presented as probability diagrams. Ages are calculated at 95% of confidence.

Figure 11: Correlation between the log of Borzatti von Löwenstern (et al., 1997), the new log (Giannandrea this work) and the archaeological levels.

Figure 12: Flakes from Cimitero di Atella unit F (a): flakes from the small tool reduction sequence. (1), (2): flint confection flakes; (3): flint resharpening flakes; (4), (5): flint notch flakes. (b) Flakes from the debitage reduction sequence. (6): coarse flint flake; (7) limestone flake proximal fragment; (8), (9) small flint flakes.

Figure 13: Diacritical analysis of a small tool, piece n° 892, F-Deb 1, dimension 47x38x12 mm. (a): Order and direction of removals; (b): Schematic description of the phases. The piece is a coarse flint flake, with a fresh overall physical state and a slight polish. The presence of partial cortex and the series of first removals (1 to 6) indicate that the flake (7) comes from the initial phases of core reduction with partial management of convexities. Phase I: 1 to 6, series of removals showing opposite and orthogonal direction with respect to the future flake (7) decorticating the block and managing the distal and lateral convexities of the debitage surface. Some of these first removals, all smaller and thinner than the future flake (7), such as, for example removal (6), can have functional lateral cutting edges. 7, detachment of thick flake, blank of future tool. Phase II: 8, 9: Orthogonal blow fracture (8) starting from lower face and adjustment (9) starting from upper face. These removals create the back of the future tool. 10 to 16: creation of TFU1 composed of trihedron and adjacent cutting edge. Two notch blows (10, 11) starting from lower face created trihedral functional part and series of small alternate retouch (12 to 16) to create a saw cutting edge. Phase III: 17 to 20: Series of scaly blows starting from upper face to create the flat surface of future TFU2. 21 to 26: Creation of TFU2 composed of trihedron. Series of small blows (21, 24, 26) push back the edge of flake, while three notch blows (22, 23, 26) create the trihedral functional part. All these blows start from the upper face. Phase IV: 27 to 31: Creation of TFU3 composed of a trihedron.

Figure 14: Techno-functional analysis of a small tool, n° 892, F-Deb 1. (a) Prehensile part (TFU p in green) composed of a flat/convex thick volume and lateral back prepared by a facture blow; transformative part (TFU t in red) made up of a trihedron and cutting-edge. (b) Prehensile part (TFU p in green) composed of a flat/convex thick volume and lateral back prepared by a facture blow; transformative part (TFU t in red) formed by a trihedron. (c) Prehensile part (TFU p in green) composed of a flat/convex thick volume and lateral back prepared by a facture blow; transformative part (TFU t in red) formed by a trihedron.

Figure 15: Large shaped tools from unit F. Due to the very poor state of preservation, it was not possible to record the angles and features of the section. (a) Shaped tool on a limestone nodule. Diacritical analysis: first phase (in grey, 1 to 10): removals linked to volumetric construction; second phase (in green, 11 to 19): series of removals to complete the prehensile part; third phase (in red, 20 to 25): series of removals to implement the transformative part. Techno-functional analysis: prehensile part (TFUp in green) consisting of a natural thick volume bordered by a natural back and a prepared back; two transformative parts (TFUt in red): TFUt 1 tip-edge and TFUt 2 a serrated edge. (b) Shaped tool on a limestone pebble. Diacritical analysis: first phase (in grey, 1 to 16) removals linked to the volumetric construction; second phase (in green, 17 to 21) series of removals to complete the prehensile part; third phase (in red, 22 to 29), series of removals to implement the transformative part. Techno-functional analysis: prehensile part (TFUp in green) consisting of a thick natural volume and a prepared lateral back; two transformative parts (TFUt in red): TFUt 1 rostrum and TFUt 2 saw edge.

References

Abruzzese, C., 2014. Il sito paleolitico di Atella (PZ) nel quadro del primo popolamento europeo: studio tecnologico dell'industria litica (Tesi di Laurea Magistrale). Università di Napoli "L'Orientale," Naples.

Abruzzese, C., Aureli, D., Rocca, R., 2016. Assessment of the Acheulean in Southern Italy: New study on the Atella site (Basilicata, Italy). Quaternary International, The first peopling of Europe and technological change during the Lower-Middle Pleistocene transition 393, 158–168. https://doi.org/10.1016/j.quaint.2015.06.005

Altamura, F., Bennett, M.R., Marchetti, L., Melis, R.T., Reynolds, S.C., Mussi, M., 2020. Ichnological and archaeological evidence from Gombore II OAM, Melka Kunture, Ethiopia: An integrated approach to reconstruct local environments and biological presences between 1.2 and 0.85 Ma. Quaternary Science Reviews 244, 106506. https://doi.org/10.1016/j.quascirev.2020.106506

997 Anketell, J.M., Cegla, J., Dzulynski, S., 1969. Unconformable surfaces formed in the absence of
998 current erosion. Geologica Romana 8, 41–46.
999 Aranguren, B., Grimaldi, S., Benvenuti, M., Capalbo, C., Cavanna, F., Cavulli, F., Ciani, F.,
1000 Comencini, G., Giuliani, C., Grandinetti, G., Mariotti Lippi, M., Masini, F., Mazza, P.P.A.,
1001 Pallecchi, P., Santaniello, F., Savorelli, A., Revedin, A., 2019. Poggetti Vecchi (Tuscany, Italy): A
1002 late Middle Pleistocene case of human–elephant interaction. Journal of Human Evolution 133, 32–
1003 60. https://doi.org/10.1016/j.jhevol.2019.05.013
1004 Arzarello, M., Pavia, G., Peretto, C., Petronio, C., Sardella, R., 2012. Evidence of an Early Pleistocene
1005 hominin presence at Pirro Nord (Apricena, Foggia, southern Italy): P13 site. Quaternary
1006 International, The genus Homo from Africa to Europe: evolution of terrestrial ecosystems and
1007 dispersal routes 267, 56–61. https://doi.org/10.1016/j.quaint.2011.01.042
1008 Aureli, D., Contardi, A., Giaccio, B., Jicha, B., Lemorini, C., Madonna, S., Magri, D., Marano, F.,
1009 Milli, S., Modesti, V., Palombo, M.R., Rocca, R., 2015. Palaeoloxodon and Human Interaction:
1010 Depositional Setting, Chronology and Archaeology at the Middle Pleistocene Ficoncella Site
1011 (Tarquinia, Italy). PLOS ONE 10, e0124498. https://doi.org/10.1371/journal.pone.0124498
1012 Aureli, D., Rocca, R., Lemorini, C., Modesti, V., Scaramucci, S., Milli, S., Giaccio, B., Marano, F.,
1013 Palombo, M.R., Contardi, A., 2016. Mode 1 or mode 2? “Small tools” in the technical variability
1014 of the European Lower Palaeolithic: The site of Ficoncella (Tarquinia, Lazio, central Italy).
1015 Quaternary International, The first peopling of Europe and technological change during the Lower-
1016 Middle Pleistocene transition 393, 169–184. https://doi.org/10.1016/j.quaint.2015.07.055Barral,
1017 L., Simone, S., 1983. Le bassin fluvio-lacustre de Venosa (Basilicate, Italie). Bull. Mus. anthropol.
1018 préhist. Monaco 5–19.
1019 Benvenuti, M., Bahain, J.-J., Capalbo, C., Capretti, C., Ciani, F., D’Amico, C., Esu, D., Giachi, Gi.,
1020 Giuliani, C., Gliozzi, E., Lazzeri, S., Macchioni, N., Lippi, M.M., Masini, F., Mazza, P.P.A.,
1021 Pallecchi, P., Revedin, A., Savorelli, A., Spadi, M., Sozzi, L., Vietti, A., Voltaggio, M., Aranguren,
1022 B., 2017. Paleoenvironmental context of the early Neanderthals of Poggetti Vecchi for the late

middle Pleistocene of Central Italy. Quaternary Research 88, 327–344. https://doi.org/10.1017/qua.2017.51

Blanc, A.C., 1953. Venosa, gisement à industrie tayacienne et micoquienne de Loreto. IV Congr. Intern. INQUA 63–68.

Boëda, É., 2013. Techno-logique & technologie, @rchéo-éditions. ed. Prigonrieux.

Boëda, É., Geneste, J.-M., Meignen, L., 1990. Identification de chaînes opératoires lithiques du Paléolithique ancien et moyen. Paléo 2, 43–80.

Bon, M., Piccoli, G., Sala, B., 1992. La fauna pleistocenica della breccia di Slivia (Carso triestino) nella collezione del Museo Civico di Storia Naturale di Trieste. Atti Mus. Civico Storia Nat. Trieste 44, 33–51.

Borzatti von Löwenstern, E., 1985. Sulle rive di un lago scomparso. L'Universo, Firenze.

Borzatti von Löwenstern, E., 1998. Il Bacino di Atella nella Preistoria. Studi per l'ecologia del Quaternario 7–39.

Borzatti von Löwenstern, E., 2005. Il sito Acheuleano antico del Cimitero di Atella: gli strati alti del sedimento preistorico. Studi per l'ecologia del Quaternario 7–20.

Borzatti von Löwenstern, E., 2011. L'antico lago di Atella: verso la fine di un ambiante geografico. Studi per l'ecologia del Quaternario 57.

Borzatti von Löwenstern, E., Sozzi, M., 1994. Prime ipotesi paleogeografiche sul sito acheuleano del Cimitero di Atella. Studi per l'ecologia del Quaternario 16.

Borzatti von Löwenstern, E., Sozzi, M., 2001. Il Bacino di Atella, 10.000 strumenti di pietra. Libria, Melfi.

Borzatti von Löwenstern, E., Vianello, F., 1990. Nuove ricerche a Masseria Palladino nel Bacino di Atella (Filiano-PZ). Studi per l'ecologia del Quaternario 12, 31.

Borzatti von Löwenstern, E., Vianello, F., 1989. L'Acheuleano antico di Masseria Palladino nel Bacino di Atella (Potenza). Studi per l'ecologia del Quaternario 11, 9.

Borzatti von Löwenstern, E., Sozzi, M., Vannucci, S., Vianello, F., 1990. L'acheuleano del cimitero

1050 di Atella. Prime indagini sulla stratigrafia del sedimento e sulle industrie litiche. Studi per
1051 l'ecologia del Quaternario 12, 9–30.
1052 Borzatti von Löwenstern, E., Palchetti, A., Sozzi, M., Maestrini, M., 1997. Témoignages de
1053 l'Acheuléen inférieur en Italie méridionale : Le gisement du Cimitero di Atella (Basilicata).
1054 L'Anthropologie 101, 617–638.
1055 Borzatti von Löwenstern, E., Fabiano, M., Secci, M.M., Sozzi, M., 1998. Paleoenvironmental
1056 investigations on the Acheulean site at the Cimitero di Atella (Potenza, Southern Italy). Atti del
1057 XIII Congr. UISPP, Forlì.
1058 Boschian, G., Saccà, D., 2015. In the elephant, everything is good: Carcass use and re-use at Castel
1059 di Guido (Italy). Quaternary International, The Origins of Recycling: A Paleolithic Perspective
1060 361, 288–296. https://doi.org/10.1016/j.quaint.2014.04.030
1061 Boschin, F., Rocca, R., Aureli, D., 2018. New archaeozoological and taphonomic analysis on macro-
1062 and megafauna remains from the Lower Palaeolithic site of Ficoncella (Tarquinia, Central Italy).
1063 Quaternaire. Revue de l'Association française pour l'étude du Quaternaire 13–20.
1064 Breda, M., Lister, A.M., 2013. *Dama roberti*, a new species of deer from the early Middle Pleistocene
1065 of Europe, and the origins of modern fallow deer. Quaternary Science Reviews 69, 155–167.
1066 https://doi.org/10.1016/j.quascirev.2013.01.029
1067 Brennan, B, Lyons, R, Phillips, S. 1991. Attenuation of alpha particle track dose for spherical grains.
1068 Nuclear Tracks Radiation Measurements 18, 249-253.
1069 Brennan, B. 2003. Beta doses to spherical grains. Radiation Measurements 37, 299- 303.
1070 Burdukiewicz, J.M., Ronen, A., 2003. Lower Palaeolithic Small Tools in Europe and the Levant.
1071 British Archaeological Reports, Oxford.
1072 Caloi L., Palombo M.R., 1979. La fauna quaternaria di Venosa: bovidi. Boll. Serv. Geol. Ital. 100,
1073 101–140.
1074 Cassoli, F., Di Stefano, G., Tagliacozzo, A., 1999. I Vertebrati dei livelli superiori (Alfa ed A) della
1075 serie stratigrafica di Notarchirico, in: Piperno, M. (Ed.), Notarchirico. Un Sito Del Pleistocene

Medio-Antico Nel Bacino Di Venosa (Basilicata). Osana edizione, Venosa, pp. 361–438.

Ciolli, N., 1997. *Elephas antiquus* Falconer & Cautley del Cimitero di Atella (Pz). Studi per l'ecologia del Quaternario 25–34.

Croitor, R., 2018. Plio-Pleistocene deer of western palearctic: taxonomy, systematics, phylogeny. Institute of Zoology of the Academy of Sciences of Moldova, Chişinău.

Clark, P.U., Archer, D., Pollard, D., Blum, J.D., Rial, J.A., Brovkin, V., Mix, A.C., Pisias, N.G., Roy, M., 2006. The middle Pleistocene transition: characteristics, mechanisms, and implications for long-term changes in atmospheric pCO2. Quaternary Science Reviews, Critical Quaternary Stratigraphy 25, 3150–3184. https://doi.org/10.1016/j.quascirev.2006.07.008

Crovetto, C., 1993. Le Paléolithique inférieur de Loreto (Venosa, Basilicate, Italie). Bulletin du Musée d'anthropologie préhistorique de Monaco 31–57.

Crovetto, C., Ferrari, M., Peretto, C., Longo, L., Vianello, F., 1994. The carinated denticulates from the Paleolithic site of Isernia La Pineta (Molise, Central Italy): Tools or flaking waste? The results of the 1993 lithic experiments. Human Evolution 9, 175–207.

Weyer, L.D., Pérez, A., Hoguin, R., Forestier, H., Boëda, E., 2022. Time, memory and alterity in prehistoric lithic technology: Synthesis and perspectives of the French technogenetic approach. Journal of Lithic Studies 9, 46 p.-46 p. https://doi.org/10.2218/jls.7020

Despriée, J., Moncel, M.-H., Arzarello, M., Courcimault, G., Voinchet, P., Bahain, J.-J., Falguères, C., 2018. The 1-million-year-old quartz assemblage from Pont-de-Lavaud (Centre, France) in the European context. Journal of Quaternary Science 33, 639–661. https://doi.org/10.1002/jqs.3042

Di Muro, A., 1999. Inquadramento tefrostratigrafico del sito acheuleano del Cimitero di Atella (Basilicata-Italia). Studi per l'ecologia del Quaternario 7–14.

Di Stefano, G., Pandolfi, L., Petronio, C., Salari, L., 2015. The morphometry and the occurrence of *Cervus elaphus* (Mammalia, Cervidae) from the Late Pleistocene of the Italian peninsula. Riv. Ital. Paleontol. Stratigr. 121(1), 103–120.

Di Stefano, G., Petronio, C., 2002. Systematics and evolution of the Eurasian Plio-Pleistocene tribe

1102 Cervini (Artiodactyla, Mammalia). Geol. Romana 36, 311–334.
1103 Duval, M., Guilarte, V., 2015. ESR dosimetry of optically bleached quartz grains extracted from Plio-
1104 quaternary sediment: evaluating some key aspects of the ESR signal associated to the Ti-center.
1105 Radiation Measurement 78, 28–41.
1106 Duveau, J., Berillon, G., Verna, C., Laisné, G., Cliquet, D., 2019. The composition of a Neandertal
1107 social group revealed by the hominin footprints at Le Rozel (Normandy, France). PNAS 116,
1108 19409–19414. https://doi.org/10.1073/pnas.1901789116
1109 Esattore, B., Saggiomo, L., Sensi, M., Francia, V., Cherin, M., 2022. Tell me what you eat and I'll tell
1110 you…where you live: an updated review of the worldwide distribution and foraging ecology of
1111 the fallow deer (Dama dama). Mamm Biol. https://doi.org/10.1007/s42991-022-00250-6
1112 Franzen, J.L., Gliozzi, E., Jellinek, T., Scholger, R., Weidenfeller, M., 2000. Die spätaltpleistozäne
1113 Fossillagerstätte Dorn-Dürkheim 3 und ihre Bedeutung für die Rekonstruktion der Entwicklung
1114 des rheinischen Flußsystems. Senckenbergiana lethaea 80, 305–353.
1115 https://doi.org/10.1007/BF03043674
1116 Fisher, R.V., Schmincke, H.-U., 2012. Pyroclastic Rocks. Springer.
1117 García-Medrano, P., Ollé, A., Mosquera, M., Cáceres, I., Díez, C., Carbonell, E., 2014. The earliest
1118 Acheulean technology at Atapuerca (Burgos, Spain): Oldest levels of the Galería site (GII Unit).
1119 Quaternary International, Environmental History of European High Mountains 353, 170–194.
1120 https://doi.org/10.1016/j.quaint.2014.03.053
1121 Giannandrea, P., 2009. Evoluzione sedimentaria della successione alluvionale e lacustre quaternaria
1122 del Bacino di Venosa (Italia meridionale). Alpine and Mediterranean Quaternary 22, 269–290.
1123 Giannandrea, P., La Volpe, L., Principe, C., Schiattarella, M., 2006. Unità stratigrafiche a limiti
1124 inconformi e storia evolutiva del vulcano medio-pleistocenico di Monte Vulture (Appennino
1125 meridionale, Italia). Bollettino-Società Geologica Italiana 125, 67.
1126 Giannandrea, P., Marino, M., Romeo, M., Schiattarella, M., 2014. Pliocene to Quaternary evolution
1127 of the Ofanto Basin in southern Italy: an approach based on the unconformity-bounded

1128 stratigraphic units. IJG 133, 27–44. https://doi.org/10.3301/IJG.2013.11
1129 Gebert, C., Verheyden-Tixier, H., 2001. Variations of diet composition of Red Deer (Cervus elaphus
1130 L.) in Europe. Mammal Review 31, 189–201. https://doi.org/10.1111/j.1365-2907.2001.00090.x
1131 Gibert, L., Alfaro, P., García-Tortosa, F.J., Scott, G., 2011. Superposed deformed beds produced by
1132 single earthquakes (Tecopa Basin, California): Insights into paleoseismology. Sedimentary
1133 Geology, Recognising triggers for soft-sediment deformation: Current understanding and future
1134 directions 235, 148–159. https://doi.org/10.1016/j.sedgeo.2010.08.003
1135 Gliozzi, E., Abbazzi, L., Argenti, P., Azzaroli, A., Caloi, L., Barbato, L.C., Stefano, G.D., Esu, D.,
1136 Ficcarelli, G., Girotti, O., Kotsakis, T., Masini, F., Mazza, P., Mezzabotta, C., Palombo, M.R.,
1137 Petronio, C., Rook, L., Sala, B., Sardella, R., Zanalda, E., Torre, D., 1997. Biochronology of
1138 selected mammals, molluscs and ostracods from the middle Pliocene to the late Pleistocene in
1139 Italy. The state of the art. Rivista Italiana di Paleontologia e Stratigrafia 103.
1140 https://doi.org/10.13130/2039-4942/5299
1141 Grifoni, R., Tozzi, C., 2006. L'émergence des identités culturelles au Paléolithique inférieur : le cas
1142 de l'Italie. Comptes Rendus Palevol, 5, 137–148.
1143 Grimaldi, S., Santaniello, F., Angelucci, D.E., Bruni, L., Parenti, F., 2020. A Techno-Functional
1144 Interpretation of the Lithic Assemblage from Fontana Ranuccio (Anagni, Central Italy): an Insight
1145 into a MIS 11 Human Behaviour. J Paleo Arch. https://doi.org/10.1007/s41982-020-00064-3
1146 Grün, R., 1994. A cautionary note: use of the "water content" and "depth for cosmic ray dose rate" in
1147 AGE and DATA. Ancient TL 12, 50- 51.
1148 Guérin, G., Mercier, N., Adamiec, G., 2011. Dose-rate conversion factors: update. Ancient TL, 29, 5-
1149 8.
1150 Guillou H, Scao V., Nomade S., 2018. 40Ar/39Ar age of cryptochron C2r.2r-1 as recorded in a lava
1151 sequence within the Ko'olau volcano (Hawaii, USA). Quaternary Geochronology 43,91–101. doi
1152 : 10.1016/j.quageo.2017.10.005
1153 Head, M.J., Gibbard, P.L., 2015. Early–Middle Pleistocene transitions: Linking terrestrial and marine

realms. Quaternary International, The Jaramillo Subchron and the Early-Middle Pleistocene transition in continental records from a multidisciplinary perspective 389, 7–46. https://doi.org/10.1016/j.quaint.2015.09.042

Iannucci, A., Mecozzi, B., Sardella, R., Iurino, D.A., 2021a. The extinction of the giant hyena Pachycrocuta brevirostris and a reappraisal of the Epivillafranchian and Galerian Hyaenidae in Europe: Faunal turnover during the Early–Middle Pleistocene Transition. Quaternary Science Reviews 272, 107240. https://doi.org/10.1016/j.quascirev.2021.107240

Iannucci, A., Mecozzi, B., Sardella, R., 2021b. Large Mammals from the Middle Pleistocene (Mis 11) site of Fontignano 2 (Rome, Central Italy), with an overview of "San Cosimato" assemblages. Alpine and Mediterranean Quaternary 34, 155–164. https://doi.org/10.26382/AMQ.2021.07

Inizan, M.-L., Reduron-Ballinger, M., Roche, H., Tixier, J., 1999. Technology and Terminology of Knapped Stone, Préhistoire de la Pierre Taillée. Éditions du CREP, Nanterre.

Iurino, D.A., Mecozzi, B., Iannucci, A., Moscarella, A., Strani, F., Bona, F., Gaeta, M., Sardella, R., 2022. A Middle Pleistocene wolf from central Italy provides insights on the first occurrence of Canis lupus in Europe. Sci Rep 12, 2882. https://doi.org/10.1038/s41598-022-06812-5

Konidaris, G.E., Athanassiou, A., Tourloukis, V., Thompson, N., Giusti, D., Panagopoulou, E., Harvati, K., 2018. The skeleton of a straight-tusked elephant (Palaeoloxodon antiquus) and other large mammals from the Middle Pleistocene butchering locality Marathousa 1 (Megalopolis Basin, Greece): preliminary results. Quaternary International, The Gates of Europe 497, 65–84. https://doi.org/10.1016/j.quaint.2017.12.001

Laurent, M., Falguères, C., Bahain, J-J., Rousseau, L., Van Vliet-Lanoë, B. 1998. ESR dating of quartz extracted from Quaternary and Neogene sediments: method, potential and actual limits. Quaternary Science Reviews 17, 1057-1061.

Lepot, M., 1993. Approche techno-fonctionnelle de l'outillage lithique Moustérien : essai de classification des parties actives en terme d'efficacité technique (Mémoire de Maîtrise). Université Paris X Nanterre, Nanterre.

1180 Lhomme, V., 2007. Tools, space and behaviour in the Lower Palaeolithic: discoveries at Soucy in the
1181 Paris basin. Antiquity 81, 536–554.
1182 Lee, J.Y., Marti, K., Severinghaus, J.P., Kawamura, K., Hee-Soo, Y., Lee, J.B., Kim, J.S., 2006. A
1183 redetermination of the isotopic abundances of atmospheric Ar. Geochimica et Cosmochimica Acta
1184 70, 4507-4512. doi: 10.1016/j.gca.2006.06.1563
1185 Longo, L., Peretto, C., Sozzi, M., Vannucci, S., Leroy-Prost, C., 1997. Artefacts, outils ou supports
1186 épuisés ? Une nouvelle approche pour l'étude des industries du Paléolithique ancien : Le cas
1187 d'Isernia La Pineta (Molise, Italie centrale). L'Anthropologie 101, 579–596.
1188 Ludwig K. R., 2003. Isoplot 3.0, a geochronological toolkit for Microsoft Excel. Berkeley
1189 Geochronology Center Special Publication, 4, 71p.
1190 Maslin, M.A., Brierley, C.M., 2015. The role of orbital forcing in the Early Middle Pleistocene
1191 Transition. Quaternary International, The Jaramillo Subchron and the Early-Middle Pleistocene
1192 transition in continental records from a multidisciplinary perspective 389, 47–55.
1193 https://doi.org/10.1016/j.quaint.2015.01.047
1194 Magri, D., Rita, F., 2015. Archaeopalynological Preparation Techniques.https://doi.org/10.1007/978-
1195 3-319-19944-3_27
1196 Margari, V., Roucoux, K., Magri, D., Manzi, G., Tzedakis, P.C., 2018. The MIS 13 interglacial at
1197 Ceprano, Italy, in the context of Middle Pleistocene vegetation changes in southern Europe.
1198 Quaternary Science Reviews 199, 144–158. https://doi.org/10.1016/j.quascirev.2018.09.016
1199 Martínez-Navarro, B., Rook, L., Papini, M., Libsekal, Y., 2010. A new species of bull from the Early
1200 Pleistocene paleoanthropological site of Buia (Eritrea): Parallelism on the dispersal of the genus
1201 Bos and the Acheulian culture. Quaternary International, Quaternary Changes of Mammalian
1202 Communities Across and Between Continents 212, 169–175.
1203 https://doi.org/10.1016/j.quaint.2009.09.003
1204 Mayoral, E., Díaz-Martínez, I., Duveau, J., Santos, A., Ramírez, A.R., Morales, J.A., Morales, L.A.,
1205 Díaz-Delgado, R., 2021. Tracking late Pleistocene Neandertals on the Iberian coast. Sci Rep 11,

4103. https://doi.org/10.1038/s41598-021-83413-8

Mecozzi, B., Iannucci, A., Sardella, R., Curci, A., Daujeard, C., Moncel, M.-H., 2021a. *Macaca* ulna from new excavations at the Notarchirico Acheulean site (Middle Pleistocene, Venosa, southern Italy). Journal of Human Evolution 153, 102946. https://doi.org/10.1016/j.jhevol.2020.102946

Mecozzi, B., Bellucci, L., Giustini, F., Iannucci, A., Iurino, D.A., Mazzini, I., Strani, F., Sardella, R., 2021b. A reappraisal of the Pleistocene mammals from the karst infilling deposits of the Maglie area (Lecce, Apulia, Southern Italy). Rivista Italiana di Paleontologia e Stratigrafia 127. https://doi.org/10.13130/2039-4942/15776

Mecozzi, B., Iannucci, A., Mancini, M., Sardella, R., 2021c. Redefining Ponte Molle (Rome, Central Italy): an important locality for Middle Pleistocene mammal assemblages of Europe. Alpine and Mediterranean Quaternary 34, 131–154. https://doi.org/10.26382/AMQ.2021.09

Mercier, N., Falguères, C., 2007. Field gamma dose-rate measurement with a NaI(Tl) detector: reevaluation of the "threshold" technique. Ancient TL, 25,1.

Miall, A.D., 1978. Tectonic setting and syndepositional deformation of molasse and other nonmarine-paralic sedimentary basins. Can. J. Earth Sci. 15, 1613–1632. https://doi.org/10.1139/e78-166

Michel, V., Shen, C.-C., Woodhead, J., Hu, H.-M., Wu, C.-C., Moullé, P.-É., Khatib, S., Cauche, D., Moncel, M.-H., Valensi, P., Chou, Y.-M., Gallet, S., Echassoux, A., Orange, F., Lumley, H., 2017. New dating evidence of the early presence of hominins in Southern Europe. Scientific Reports 7, 10074. https://doi.org/10.1038/s41598-017-10178-4

Moncel, M., Schreve, D., 2016. The Acheulean in Europe: Origins, evolution and dispersal. Quaternary International, The Acheulean in Europe: origins, evolution and dispersal 411, Part B, 1–8. https://doi.org/10.1016/j.quaint.2016.08.039

Moncel, M.-H., Despriée, J., Voinchet, P., Tissoux, H., Moreno, D., Bahain, J.-J., Courcimault, G., Falguères, C., 2013. Early Evidence of Acheulean Settlement in Northwestern Europe - La Noira Site, a 700 000 Year-Old Occupation in the Center of France. PLOS ONE 8, e75529. https://doi.org/10.1371/journal.pone.0075529

1232 Moncel, M.-H., Ashton, N., Lamotte, A., Tuffreau, A., Cliquet, D., Despriée, J., 2015. The Early
1233 Acheulian of north-western Europe. Journal of Anthropological Archaeology 40, 302–331.
1234 Moncel, M.-H., Despriée, J., Voinchet, P., Courcimault, G., Hardy, B., Bahain, J.-J., Puaud, S., Gallet,
1235 X., Falguères, C., 2016. The Acheulean workshop of la Noira (France, 700 ka) in the European
1236 technological context. Quaternary International, The first peopling of Europe and technological
1237 change during the Lower-Middle Pleistocene transition 393, 112–136.
1238 https://doi.org/10.1016/j.quaint.2015.04.051
1239 Moncel, M.-H., Arzarello, M., Boëda, É., Bonilauri, S., Chevrier, B., Gaillard, C., Forestier, H.,
1240 Yinghua, L., Sémah, F., Zeitoun, V., 2018. The assemblages with bifacial tools in Eurasia (first
1241 part). What is going on in the West? Data on western and southern Europe and the Levant. Comptes
1242 Rendus Palevol, Hominins and tools. Expansion from Africa towards Eurasia / Homininés et outils.
1243 Expansions depuis l'Afrique vers l'Eurasie 17, 45–60. https://doi.org/10.1016/j.crpv.2015.09.009
1244 Moncel, M.-H., Santagata, C., Pereira, A., Nomade, S., Bahain, J.-J., Voinchet, P., Piperno, M., 2019.
1245 A biface production older than 600 ka ago at Notarchirico (Southern Italy) contribution to
1246 understanding early Acheulean cognition and skills in Europe. PLOS ONE 14, e0218591.
1247 https://doi.org/10.1371/journal.pone.0218591
1248 Moncel, M.-H., Santagata, C., Pereira, A., Nomade, S., Voinchet, P., Bahain, J.-J., Daujeard, C., Curci,
1249 A., Lemorini, C., Hardy, B., Eramo, G., Berto, C., Raynal, J.-P., Arzarello, M., Mecozzi, B.,
1250 Iannucci, A., Sardella, R., Allegretta, I., Delluniversità, E., Terzano, R., Dugas, P., Jouanic, G.,
1251 Queffelec, A., d'Andrea, A., Valentini, R., Minucci, E., Carpentiero, L., Piperno, M., 2020. The
1252 origin of early Acheulean expansion in Europe 700 ka ago: new findings at Notarchirico (Italy).
1253 Sci Rep 10, 13802. https://doi.org/10.1038/s41598-020-68617-8.
1254 Mosquera, M., Ollé, A., Saladié, P., Cáceres, I., Huguet, R., Rosas, A., Villalaín, J., Carrancho, A.,
1255 Bourlès, D., Braucher, R., Pineda, A., Vallverdú, J., 2016. The Early Acheulean technology of
1256 Barranc de la Boella (Catalonia, Spain). Quaternary International, The first peopling of Europe
1257 and technological change during the Lower-Middle Pleistocene transition 393, 95–111.

https://doi.org/10.1016/j.quaint.2015.05.005

Nehyba, S., Nývlt, D., 2014. Deposits of pyroclastic mass flows at Bibby Hill (Pliocene, James Ross Island, Antarctica). Czech Polar Reports 4, 103–122. https://doi.org/10.5817/CPR2014-2-11

Nicoud, E., 2011. Le phénomène acheuléen en Europe occidentale : Approche chronologique, technologie lithique et implications culturelles (Thèse de doctorat). Université Aix Marseille 1, Aix-en-Provence.

Nicoud, E., 2013. What does the Acheulean consist of? The example of Western Europe (MIS 16-9). Mitteilungen der Gesellschaft für Urgeschichte 22, 41–60.

Nicoud, E., Aureli, D., Pagli, M., Villa, V., Chaussé, C., Agostini, S., Bahain, J.-J., Boschian, G., Degeai, J.-P., Fusco, F., Giaccio, B., Hernandez, M., Kuzucuoglu, C., Lahaye, C., Lemorini, C., Limondin-Lozouet, N., Mazza, P., Mercier, N., Nomade, S., Pereira, A., Robert, V., Rossi, M.A., Virmoux, C., Zupancich, A., 2016. Preliminary data from Valle Giumentina Pleistocene site (Abruzzo, Central Italy): A new approach to a Clactonian and Acheulian sequence. Quaternary International, Special Issue: The Hoslteinian period in Europe (MIS 11-9) 409, Part B, 182–194. https://doi.org/10.1016/j.quaint.2015.08.080

Niespolo, E.M., Rutte, D., Deino, A. et Renne, P.R., 2017. Intercalibration and age of the Alder Creek sanidine 40Ar/39Ar standard. Quaternary Geochronology in press. http://dx.doi. org/10.1016/j.quageo.2016.09.004

Nomade, S., Gauthier, A., Guillou, H., Pastre, J.F., 2010. 40Ar/39Ar temporal framework for the Alleret maar lacustrine sequence (French Massif-Central): Volcanological and paleoclimatic implications. Quaternary Geochronology 5, 20-27.

Ollé, A., Mosquera, M., Rodríguez, X.P., de Lombera-Hermida, A., García-Antón, M.D., García-Medrano, P., Peña, L., Menéndez, L., Navazo, M., Terradillos, M., Bargalló, A., Márquez, B., Sala, R., Carbonell, E., 2013. The Early and Middle Pleistocene technological record from Sierra de Atapuerca (Burgos, Spain). Quaternary International, East meets West: First settlements and human evolution in Eurasia 295, 138–167. https://doi.org/10.1016/j.quaint.2011.11.009

1284 Orain, R., Lebreton, V., Ermolli, E.R., Combourieu-Nebout, N., Sémah, A.-M., 2013. *Carya* as
1285 marker for tree refuges in southern Italy (Boiano basin) at the Middle Pleistocene.
1286 Palaeogeography, Palaeoclimatology, Palaeoecology 369, 295–302.
1287 https://doi.org/10.1016/j.palaeo.2012.10.037
1288 Orain, R., Russo Ermolli, E., Lebreton, V., Di Donato, V., Bahain, J.-J., Sémah, A.-M., 2015.
1289 Vegetation sensitivity to local environmental factors and global climate changes during the Middle
1290 Pleistocene in southern Italy—A case study from the Molise Apennines. Review of Palaeobotany
1291 and Palynology 220, 69–77. https://doi.org/10.1016/j.revpalbo.2015.05.002
1292 Palladino, G., Giannandrea, P., Siniscalchi, A., Magri, C., Loiacono, F., 2018. Quaternary
1293 tectonostratigraphic evolution of the Vlora Basin, south-western Albania. Geological Journal 53,
1294 1698–1715. https://doi.org/10.1002/gj.2992
1295 Palma Di Cesnola, A., 2001. Il paleolitico inferiore e medio in Italia, Millenni. Museo Fiorentino di
1296 Preistoria "Paolo Graziosi," Firenze.
1297 Palombo, M.R., Ferretti, M.P., 2005. Elephant fossil record from Italy: knowledge, problems, and
1298 perspectives. Quaternary International, Studying Proboscideans: knowledge, Problems and
1299 Perspectives. Selected papers from "The world of Elephants" Congress, Rome 126–128, 107–136.
1300 https://doi.org/10.1016/j.quaint.2004.04.018
1301 Palombo, M.R., Filippi, M.L., Iacumin, P., Longinelli, A., Barbieri, M., Maras, A., 2005. Coupling
1302 tooth microwear and stable isotope analyses for palaeodiet reconstruction: the case study of Late
1303 Middle Pleistocene Elephas (Palaeoloxodon) antiquus teeth from Central Italy (Rome area).
1304 Quaternary International, Studying Proboscideans: knowledge, Problems and Perspectives.
1305 Selected papers from "The world of Elephants" Congress, Rome 126–128, 153–170.
1306 https://doi.org/10.1016/j.quaint.2004.04.020
1307 Pereira, A., Nomade, S., Voinchet, P., Bahain, J.J., Falguères, C., Garon, H., Lefèvre, D., Raynal, J.P.,
1308 Scao, V., Piperno, M., 2015. The earliest securely dated hominin fossil in Italy and evidence of
1309 Acheulian occupation during glacial MIS 16 at Notarchirico (Venosa, Basilicata, Italy). Journal of

Quaternary Science 30, 639–650.

Peretto, C., Terzani, C., Vannucci, S., Vaselli, O., Vianello, F., 1994. Le industrie litiche del giacimento paleolitico di Isernia La Pineta: la tipologia, le tracce di utilizzazione, la sperimentazione, Cosmo Iannone edizione. ed. Campobasso.

Peretto, C., Arzarello, M., Gallotti, R., Lembo, G., Minelli, A., Thun Hohenstein, U., 2004. Middle Pleistocene behavioural strategies: the contribution of Isernia La Pineta site, in: Baquedano Pérez, E., Rubio-Jara, S., Aguirre, E. (Eds.), Miscelánea En Homenaje a Emiliano Aguirre. Comunidad de Madrid, Museo Arqueológico Regional, Madrid, pp. 369–381.

Peretto, C., Arnaud, J., Moggi-Cecchi, J., Manzi, G., Nomade, S., Pereira, A., Falguères, C., Bahain, J.-J., Grimaud-Hervé, D., Berto, C., Sala, B., Lembo, G., Muttillo, B., Gallotti, R., Hohenstein, U.T., Vaccaro, C., Coltorti, M., Arzarello, M., 2015. A Human Deciduous Tooth and New 40Ar/39Ar Dating Results from the Middle Pleistocene Archaeological Site of Isernia La Pineta, Southern Italy. PLOS ONE 10, e0140091. https://doi.org/10.1371/journal.pone.0140091

Petrosino, P., Jicha, B.R., Mazzeo, F.C., Russo Ermolli, E., 2014a. A high resolution tephrochronological record of MIS 14–12 in the Southern Apennines (Acerno Basin, Italy). Journal of Volcanology and Geothermal Research 274, 34–50. https://doi.org/10.1016/j.jvolgeores.2014.01.014

Petrosino, P., Ermolli, E.R., Donato, P., Jicha, B., Robustelli, G., Sardella, R., 2014b. Using Tephrochronology and palynology to date the MIS 13 lacustrine sediments of the Mercure basin (Southern Apennines–Italy). Italian Journal of Geosciences 133, 169–186.

Pieruccini, P., Forti, L., Mecozzi, B., Iannucci, A., Yu, T.-L., Shen, C.-C., Bona, F., Lembo, G., Muttillo, B., Sardella, R., Mazzini, I., 2022. Stratigraphic reassessment of Grotta Romanelli sheds light on Middle-Late Pleistocene palaeoenvironments and human settling in the Mediterranean. Sci Rep 12, 13530. https://doi.org/10.1038/s41598-022-16906-9

Pilleyre, T., Sanzelle, S., Fain, J., Miallier, D., Montret, M., 1999. Essai de datation par thermoluminescence des depots du site acheuleen de Notarchirico, in: Piperno, M. (Ed.),

1336 Notarchirico. Un Sito Del Pleistocene Medio-Antico Nel Bacino Di Venosa (Basilicata),. Osana
1337 edizione, p. 235.
1338 Piperno, M. (Ed.), 1999. Notarchirico: un sito del Pleistocene medio antico nel bacino di Venosa.
1339 Osana edizione, Venosa.
1340 Pope, M.C., Fred Read, J., Bambach, R., Hofmann, H.J., 1997. Late Middle to Late Ordovician
1341 seismites of Kentucky, southwest Ohio and Virginia: Sedimentary recorders of earthquakes in the
1342 Appalachian basin. Geological Society of America Bulletin 109, 489–503.
1343 Prescott, J.R., Hutton, J.T., 1994. Cos3ic ray contributions to dose rates for luminescence and ESR
1344 dating: large depths and long-term time variations. Radiation Measurements, 23, 497–500.
1345 Rivals, F., Semprebon, G., Lister, A., 2012. An examination of dietary diversity patterns in Pleistocene
1346 proboscideans (Mammuthus, Palaeoloxodon, and Mammut) from Europe and North America as
1347 revealed by dental microwear. Quaternary International, Mammoths and Their Relatives 1:
1348 Biotopes, Evolution and Human Impact V International Conference, Le Puy-en-Velay, 2010 255,
1349 188–195. https://doi.org/10.1016/j.quaint.2011.05.036
1350 Rivals, F., Ziegler, R., 2018. High-resolution paleoenvironmental context for human occupations
1351 during the Middle Pleistocene in Europe (MIS 11, Germany). Quaternary Science Reviews 188,
1352 136–142. https://doi.org/10.1016/j.quascirev.2018.03.026
1353 Rocca, R., 2016. First settlements in Central Europe: Between originality and banality. Quaternary
1354 International, Special Issue: The Hoslteinian period in Europe (MIS 11-9) 409, Part B, 213–221.
1355 https://doi.org/10.1016/j.quaint.2015.08.066
1356 Rocca, R., Abruzzese, C., Aureli, D., 2016. European Acheuleans: Critical perspectives from the East.
1357 Quaternary International, The Acheulean in Europe: origins, evolution and dispersal 411, Part B,
1358 402–411. https://doi.org/10.1016/j.quaint.2016.01.025
1359 Rocca, R., Aureli, D., 2019. Cimitero di Atella. Résultats de la mission 2018. Chronique des activités
1360 archéologiques de l'École française de Rome. https://doi.org/10.4000/cefr.3329
1361 Rocca, R., Aureli, D., Abruzzese, C., 2018. Cimitero di Atella. Nouvelles recherches et valorisation

1362 d’un gisement du Paléolithique ancien en Méditerranée. Chronique des activités archéologiques
1363 de l’École française de Rome. https://doi.org/10.4000/cefr.1910
1364 Rocca, R., Boschin, F., Aureli, D., 2021. Around an elephant carcass: Cimitero di Atella and
1365 Ficoncella in the behavioural variability during the Early Middle Pleistocene in italy, in: Konidaris,
1366 G., Barkai, R., Tourloukis, V., Harvati, K. (Eds.), Human-Elephant Interactions: From Past to
1367 Present, Tübingen Paleoanthropology Book Series – Volume Contributions in Paleoanthropology.
1368 Tübingen University Press, Tübingen, pp. 287–302.
1369 Rocca, R., Da Costa, A., Germond, L., Aureli, D., 2020. Cimitero di Atella : résultats de la mission
1370 2019. Chronique des activités archéologiques de l’École française de Rome.
1371 https://doi.org/10.4000/cefr.4436
1372 Sanders, D., Ostermann, M., Kramers, J., 2009. Quaternary carbonate-rocky talus slope successions
1373 (Eastern Alps, Austria): sedimentary facies and facies architecture. Facies 55, 345.
1374 https://doi.org/10.1007/s10347-008-0175-z
1375 Santagata, C., Moncel, M.-H., Piperno, M., 2020. Bifaces or not bifaces? Role of raw materials in the
1376 Middle Pleistocene. The example of levels E-E1, B and F (610–670 ka) at Notarchirico (Italy).
1377 Journal of Archaeological Science: Reports 33, 102544.
1378 https://doi.org/10.1016/j.jasrep.2020.102544
1379 Santucci, E., Marano, F., Cerilli, E., Fiore, I., Lemorini, C., Palombo, M.R., Anzidei, A.P., Bulgarelli,
1380 G.M., 2016. Palaeoloxodon exploitation at the Middle Pleistocene site of La Polledrara di
1381 Cecanibbio (Rome, Italy). Quaternary International, VIth International Conference on Mammoths
1382 and their Relatives, Part 2 406, Part B, 169–182.
1383 https://doi.org/10.1016/j.quaint.2015.08.042Segre, A.G., 1962. Considerazioni preliminari sul
1384 paleolitico inferiore e sulla stratigrafia del bacino di Atella-Vitalba, Lucania. Quaternaria IV, 199–
1385 203.
1386 Schiattarella, M., Beneduce, P., Di Leo, P., Giano, S.I., Giannandrea, P., Principe, C., 2005. Assetto
1387 strutturale ed evoluzione morfotettonica quaternaria del vulcano del Monte Vulture (Appennino

Lucano). Bollettino-Società Geologica Italiana 124, 543.

Schiattarella, M., Giannandrea, P., Principe, C., La Volpe, L., 2016. Note Illustrative della Carta Geologica d'Italia alla scala 1:50.000 - Foglio 451 Melfi, in: Carta Geologica d'Italia Alla Scala 1:50.000. Servizio Geologico d'Italia Litografia Artistica Cartografica, Firenze.

Segre, A.G., 1957. Considerazioni preliminari sul Paleolitico inferiore e sulla stratigrafia del bacino di Atella-Vitalba (Lucania). Quaternaria IV, 199–203.

Serangeli, J., Böhner, U., Van Kolfschoten, T., Conard, N.J., 2015. Overview and new results from large-scale excavations in Schöningen. Journal of Human Evolution, Special Issue: Excavations at Schöningen: New Insights into Middle Pleistocene Lifeways in Northern Europe 89, 27–45. https://doi.org/10.1016/j.jhevol.2015.09.013

Strani, F., Bellucci, L., Iannucci, A., Iurino, D.A., Mecozzi, B., Sardella, R., 2022. Palaeoenvironments of the MIS 15 site of Cava di Breccia - Casal Selce 2 (central Italian Peninsula) and niche occupation of fossil ungulates during Middle Pleistocene interglacials. Historical Biology 34, 555–565. https://doi.org/10.1080/08912963.2021.1935920

Tourloukis, V., Thompson, N., Panagopoulou, E., Giusti, D., Konidaris, G.E., Karkanas, P., Harvati, K., 2018. Lithic artifacts and bone tools from the Lower Palaeolithic site Marathousa 1, Megalopolis, Greece: Preliminary results. Quaternary International, The Gates of Europe 497, 47–64. https://doi.org/10.1016/j.quaint.2018.05.043

Tissoux, H., Falguères C., Voinchet P., Toyoda S., Bahain J.J., Despriée J. 2007. Potential use of Ti centre in ESR dating of Fluvial Sediment. Quaternary Geochronology, 2, 1-4, 367-372

Tourloukis, V., Thompson, N., Panagopoulou, E., Giusti, D., Konidaris, G.E., Karkanas, P., Harvati, K., 2018. Lithic artifacts and bone tools from the Lower Palaeolithic site Marathousa 1, Megalopolis, Greece: Preliminary results. Quaternary International, The Gates of Europe 497, 47–64. https://doi.org/10.1016/j.quaint.2018.05.043

Toyoda, S., Falguères, C., 2003. The method to represent the ESR signal intensity of the aluminium hole centre in quartz for the purpose of dating. Adv. ESR Appl. 20, 7–10.

1414 Toyoda, S., Voinchet, P., Falguères, C., Dolo, J.M., Laurent, M., 2000. Bleaching of ESR signal by
1415 the sunlight: a laboratory experiment for establishing the ESR dating of sediments. Applied
1416 Radiation Isotopes, 52, 5, 1357–1362.
1417 van der Made, J., Rosell, J., Blasco, R., 2017. Faunas from Atapuerca at the Early–Middle Pleistocene
1418 limit: The ungulates from level TD8 in the context of climatic change. Quaternary International,
1419 What's happening now in Atapuerca? Latest research at the Sierra de Atapuerca sites 433, 296–
1420 346. https://doi.org/10.1016/j.quaint.2015.09.009
1421 van Kolfschoten, T., Parfitt, S.A., Serangeli, J., Bello, S.M., 2015. Lower Paleolithic bone tools from
1422 the 'Spear Horizon' at Schöningen (Germany). Journal of Human Evolution, Special Issue:
1423 Excavations at Schöningen: New Insights into Middle Pleistocene Lifeways in Northern Europe
1424 89, 226–263. https://doi.org/10.1016/j.jhevol.2015.09.012
1425 Villa, I.M., Buettner, A., 2009. Chronostratigraphy of Monte Vulture volcano (southern Italy):
1426 secondary mineral microtextures and 39Ar-40Ar systematics. Bull Volcanol 71, 1195.
1427 https://doi.org/10.1007/s00445-009-0294-6
1428 Villa, P., Boschian, G., Pollarolo, L., Saccà, D., Marra, F., Nomade, S., Pereira, A., 2021. Elephant
1429 bones for the Middle Pleistocene toolmaker. PLOS ONE 16, e0256090.
1430 https://doi.org/10.1371/journal.pone.0256090
1431 Voinchet, P., Bahain, J.-J., Falguères, C., Laurent, M., Dolo, J., Despriée, J., Gageonnet, R., Chaussé,
1432 C., 2004. ESR dating of quartz extracted from Quaternary sediments application to fluvial terraces
1433 system of northern France [Datation par résonance paramagnétique électronique (RPE) de quartz
1434 fluviatiles quaternaires: application aux systèmes de terrasses du nord de la France.]. Quaternaire
1435 15, 135–141. https://doi.org/10.3406/quate.2004.1761
1436 Voinchet, P., Pereira, A., Nomade, S., Falguères, C., Biddittu, I., Piperno, M., Moncel, M.-H., Bahain,
1437 J.-J., 2020. ESR dating applied to optically bleached quartz - a comparison with 40Ar/39Ar
1438 chronologies on Italian Middle Pleistocene sequences, Quaternary International, 556, 113-123.
1439 Walker, R.G., James, N.P., 1992. Facies Models: Response to Sea Level Change. Geological

1440 Association of Canada, Toronto.
1441 Zucchelli, M., 1999. Bos primigenius Bojanus del Bacino di Atella (Potenza). Studi per l'ecologia
1442 del Quaternario 19–30.
1443 Zucchelli, M., 2002. I cervidi dell'Acheuleano antico del Cimitero di Atella (Potenza). Studi per
1444 l'ecologia del Quaternario 3–17.
1445 Wright E., 2013. The history of the European aurochs (*Bos primigenius*) from the Middle Pleistocene
1446 to its extinction: an archaeological investigation of its evolution, morphological variability and
1447 response to human exploitation. PhD thesis. University of Sheffield.

Figure 1

Click here to access/download;Figure;FIG1.jpg

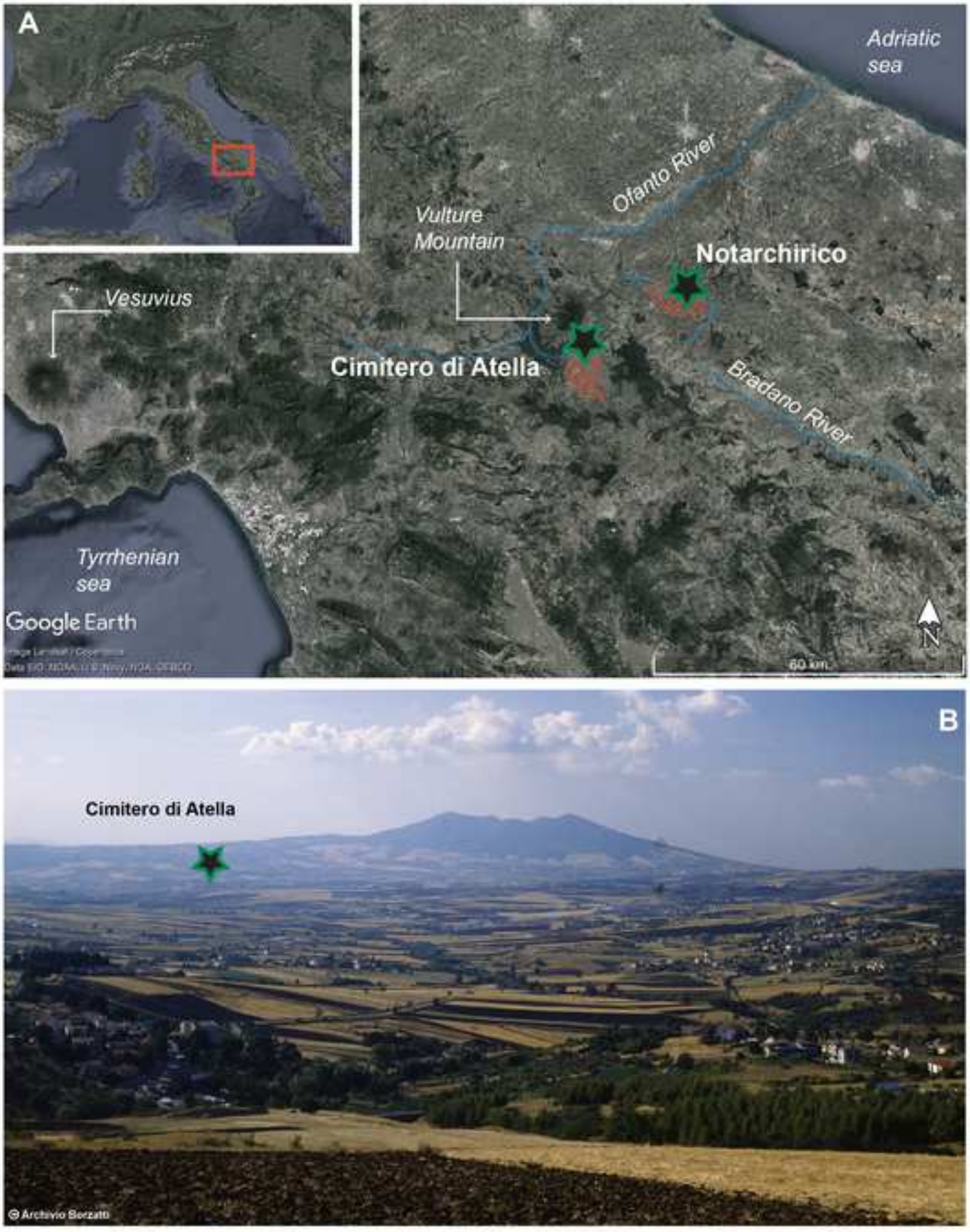

Figure 2

Click here to access/download;Figure;FIG2.jpg

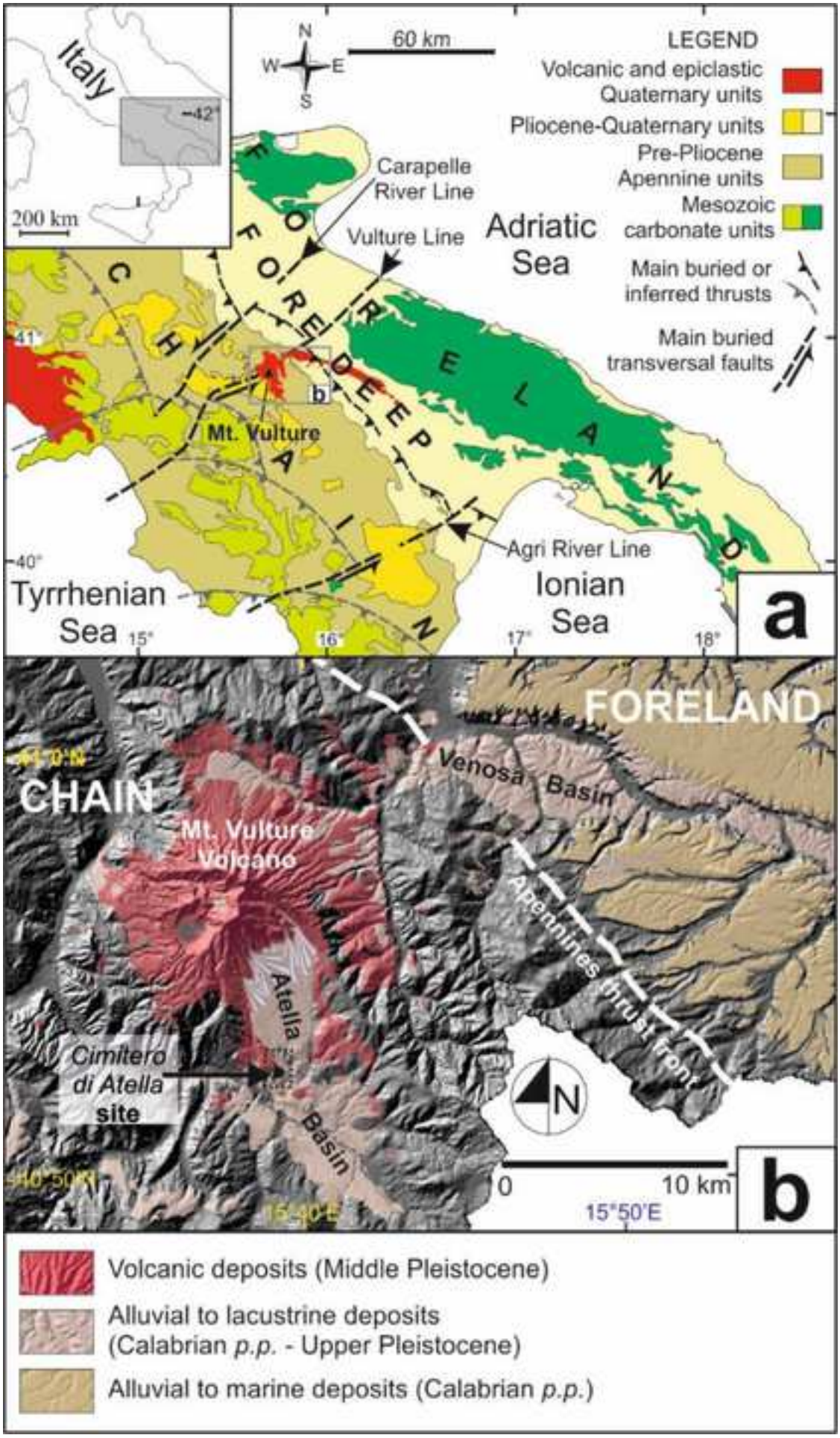

Figure 3

Click here to access/download;Figure;FIG3.jpg

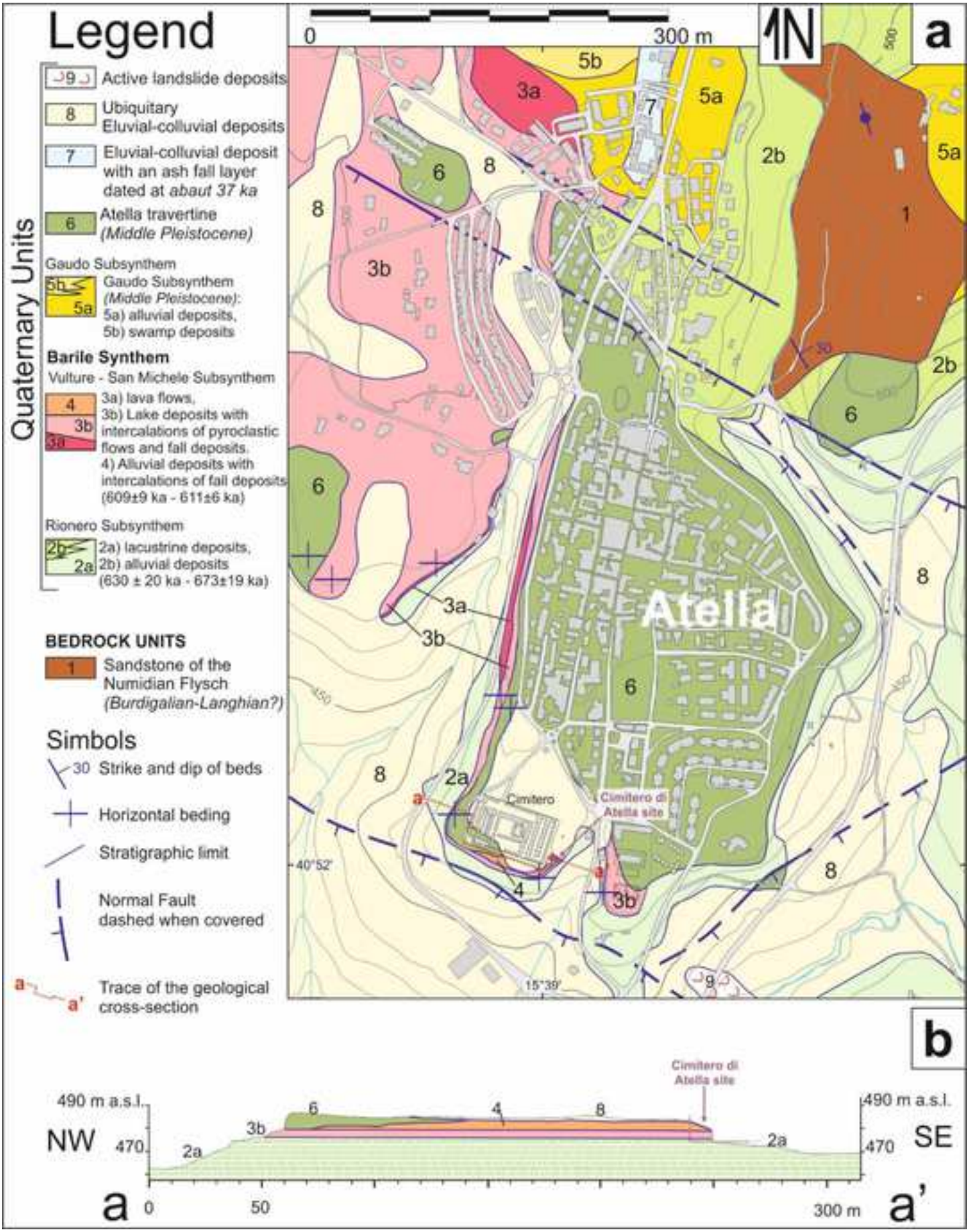

Figure 4

Click here to access/download;Figure;FIG4.jpg

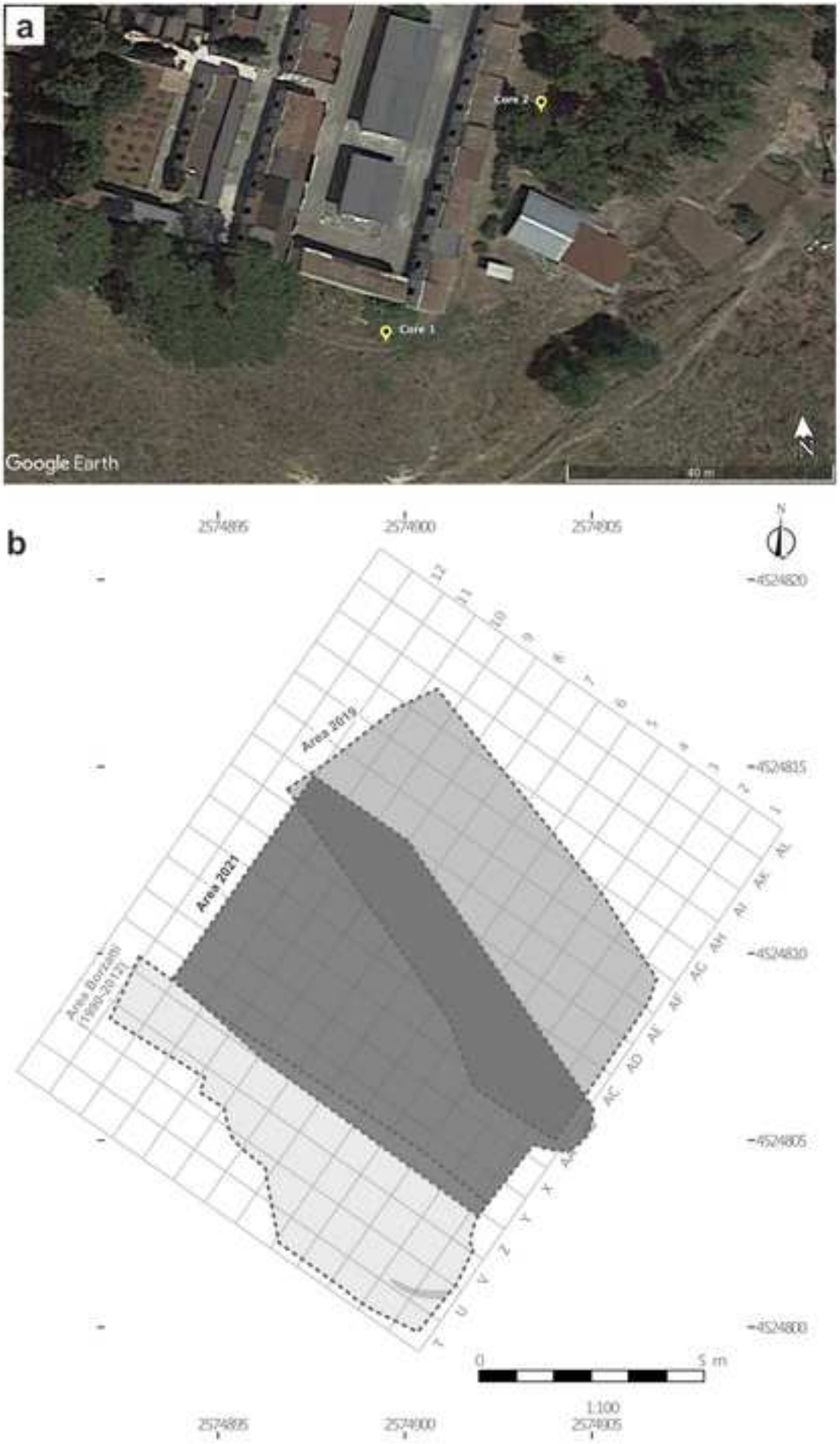

Figure 5

Click here to access/download;Figure;FIG5.jpg

Figure 6

Click here to access/download;Figure;FIG6.jpg

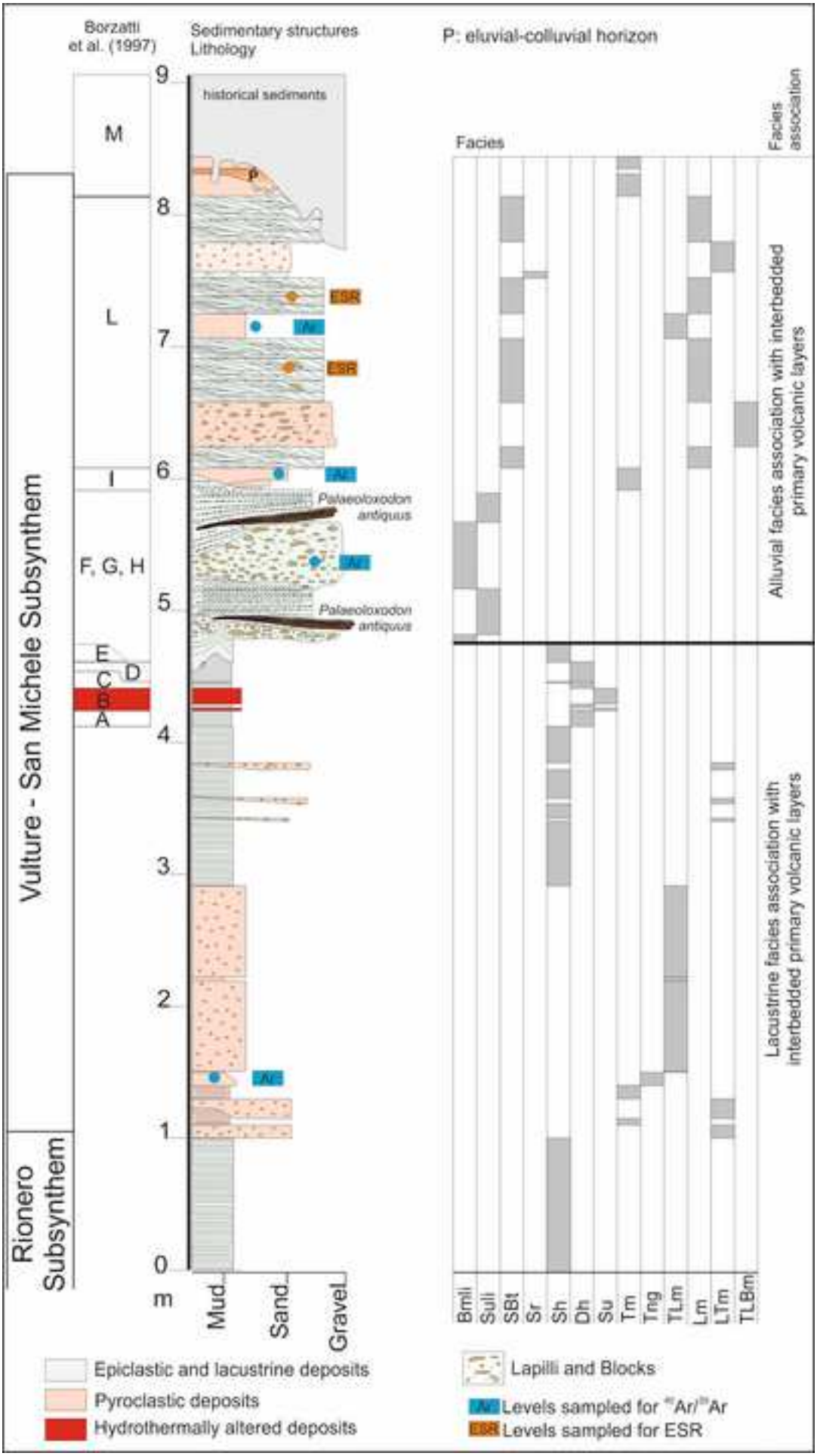

Figure 7

Click here to access/download;Figure;FIG7.jpg

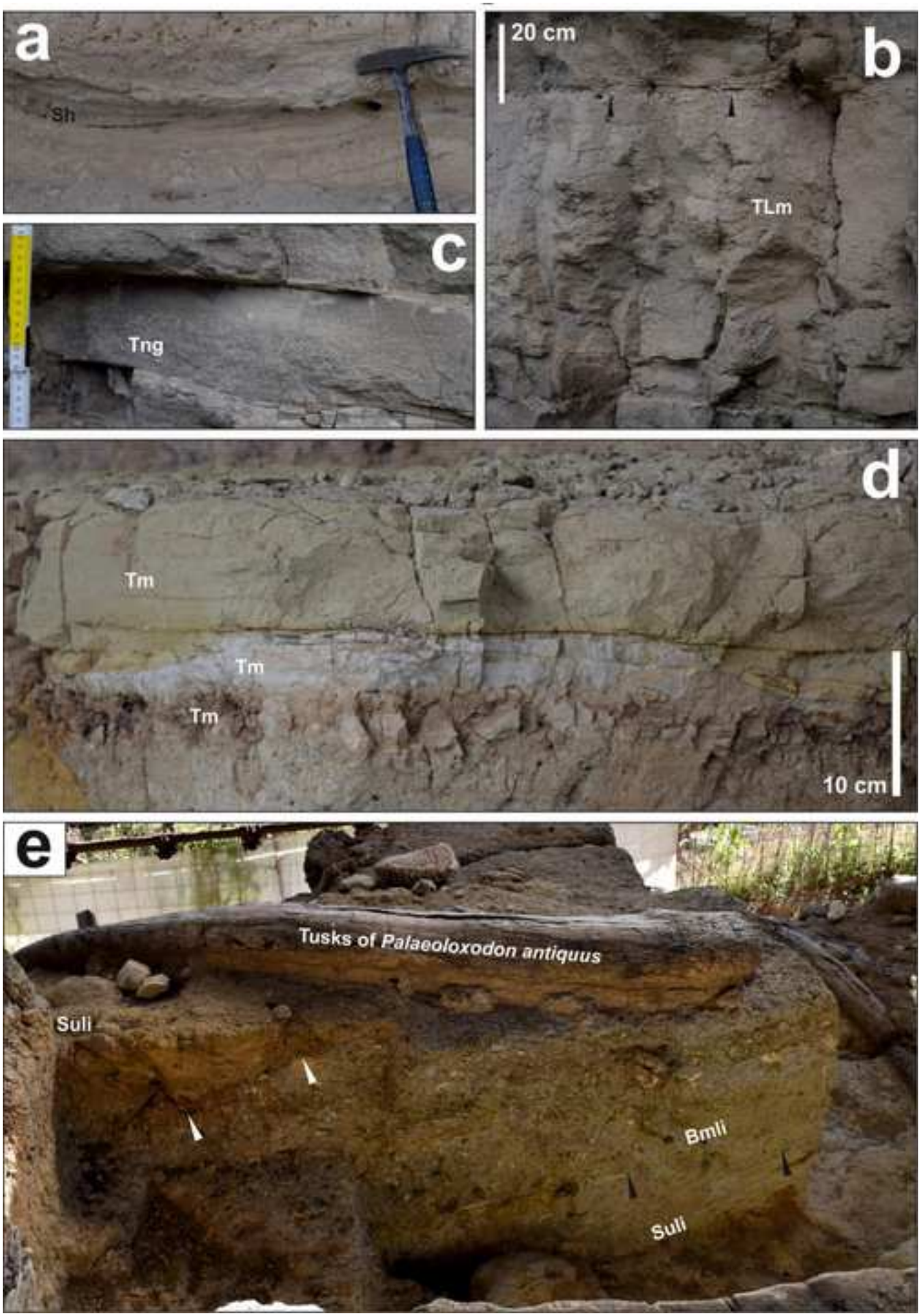

Figure 8

Click here to access/download;Figure;FIG8.jpg

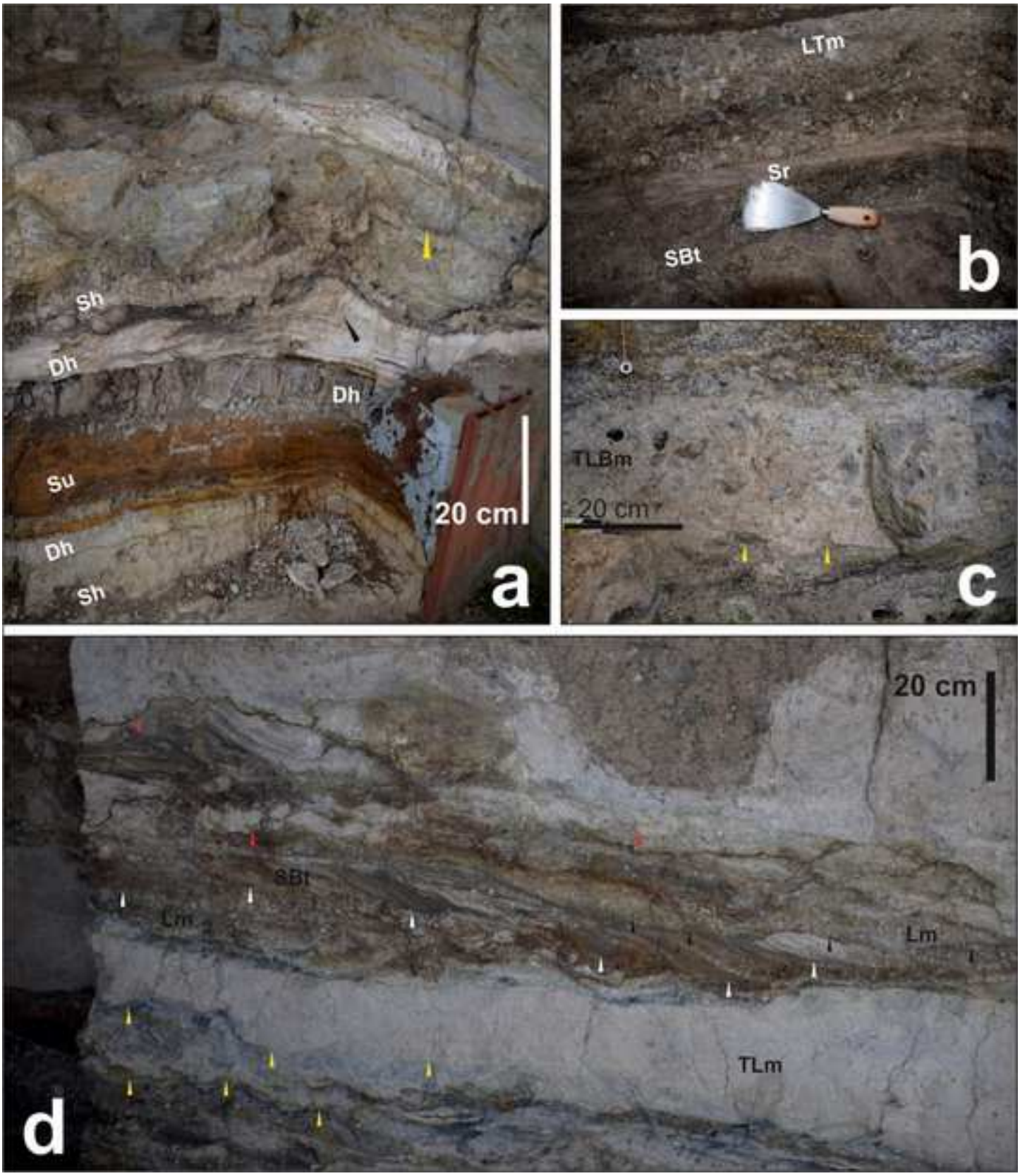

Figure 9

Click here to access/download;Figure;FIG9.jpg

Figure 10

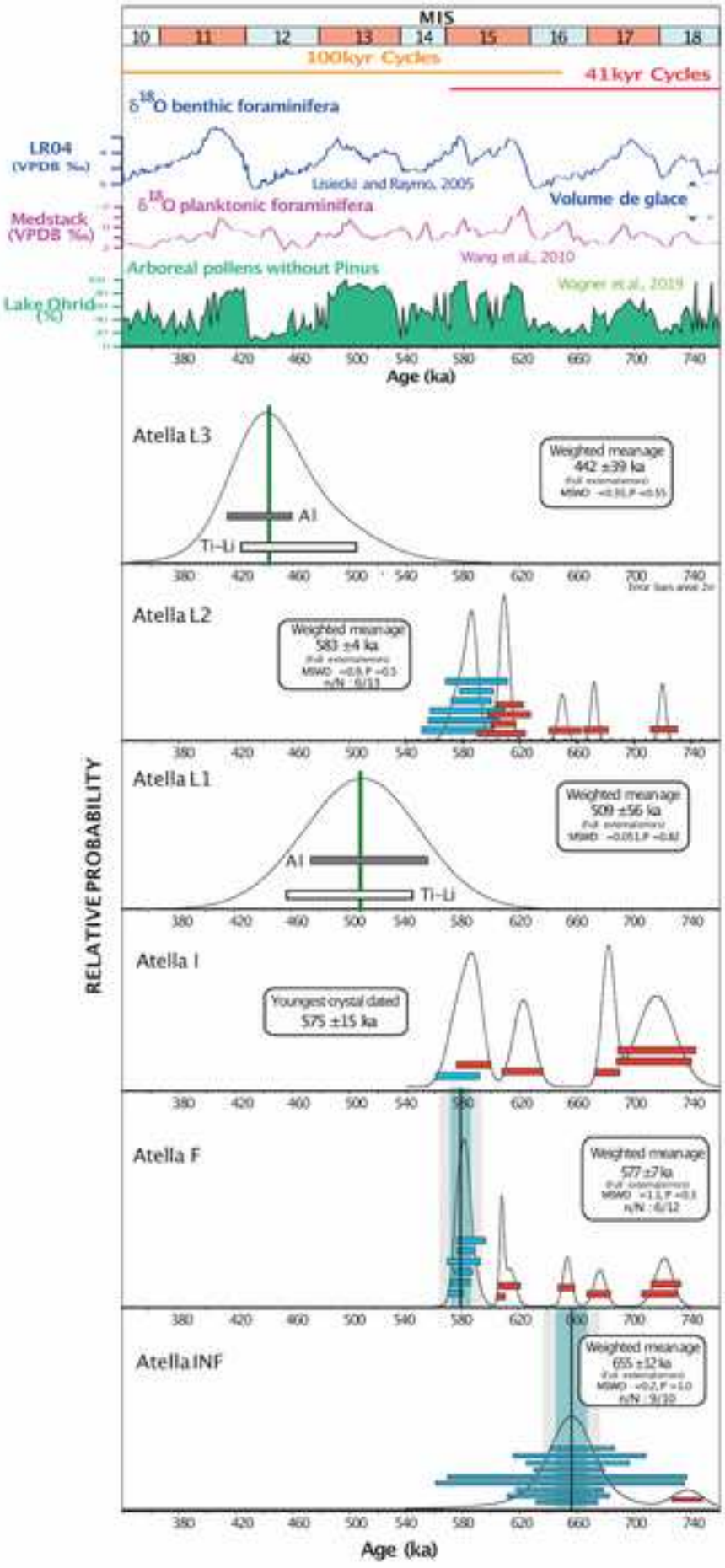

Figure 11

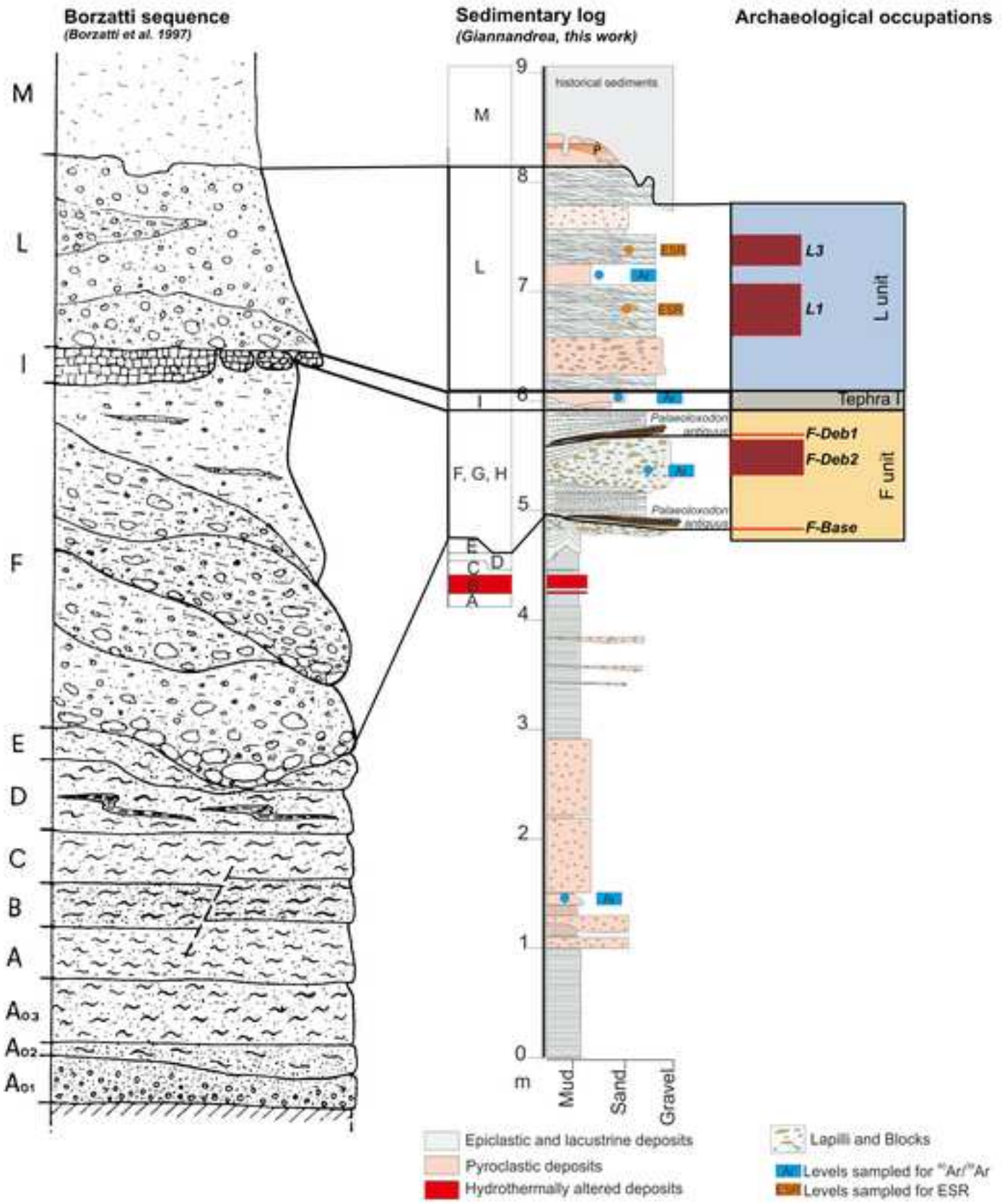

Figure 12

Click here to access/download;Figure;FIG12.jpg

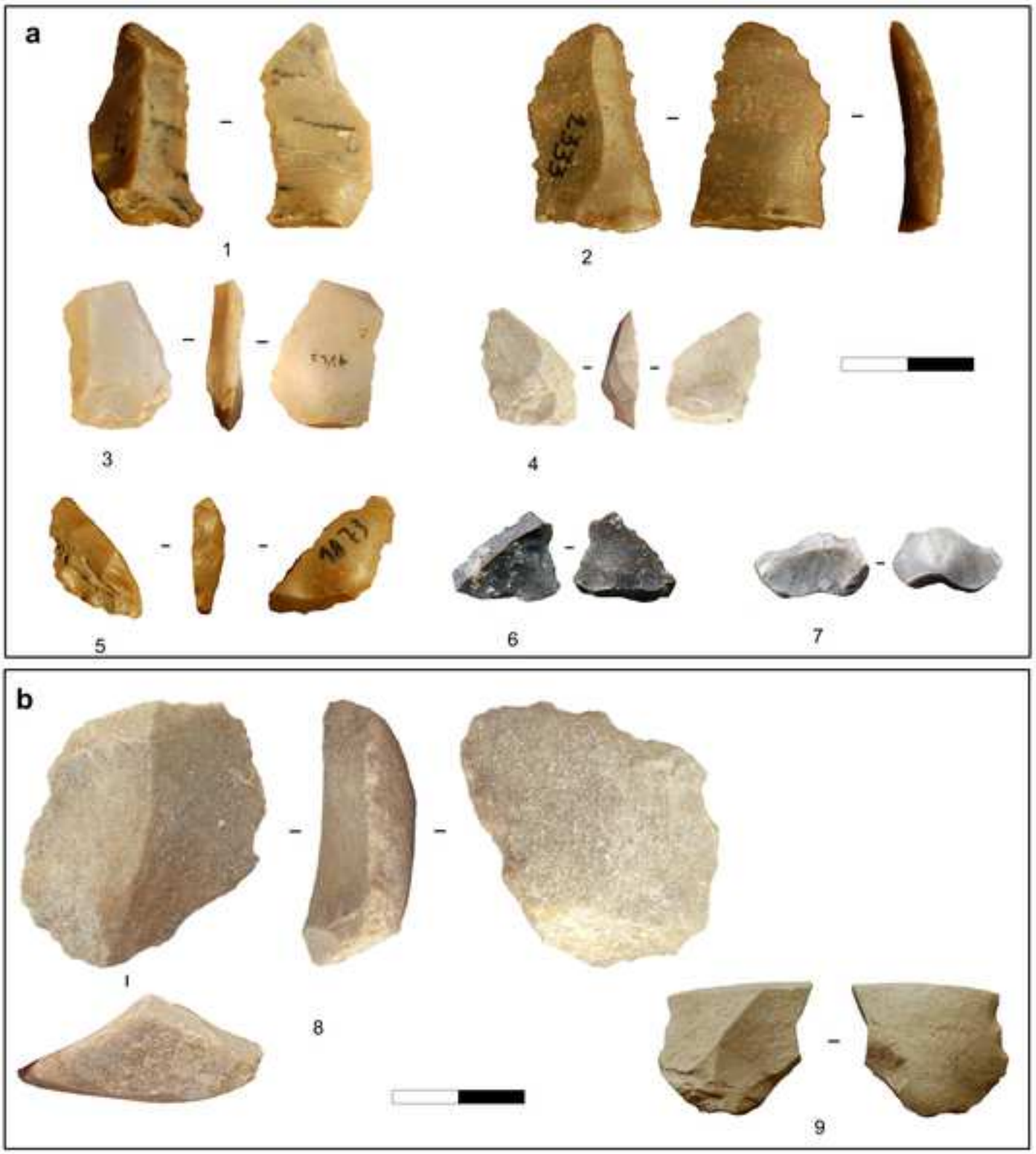

Figure 13

Click here to access/download;Figure;FIG13.jpg

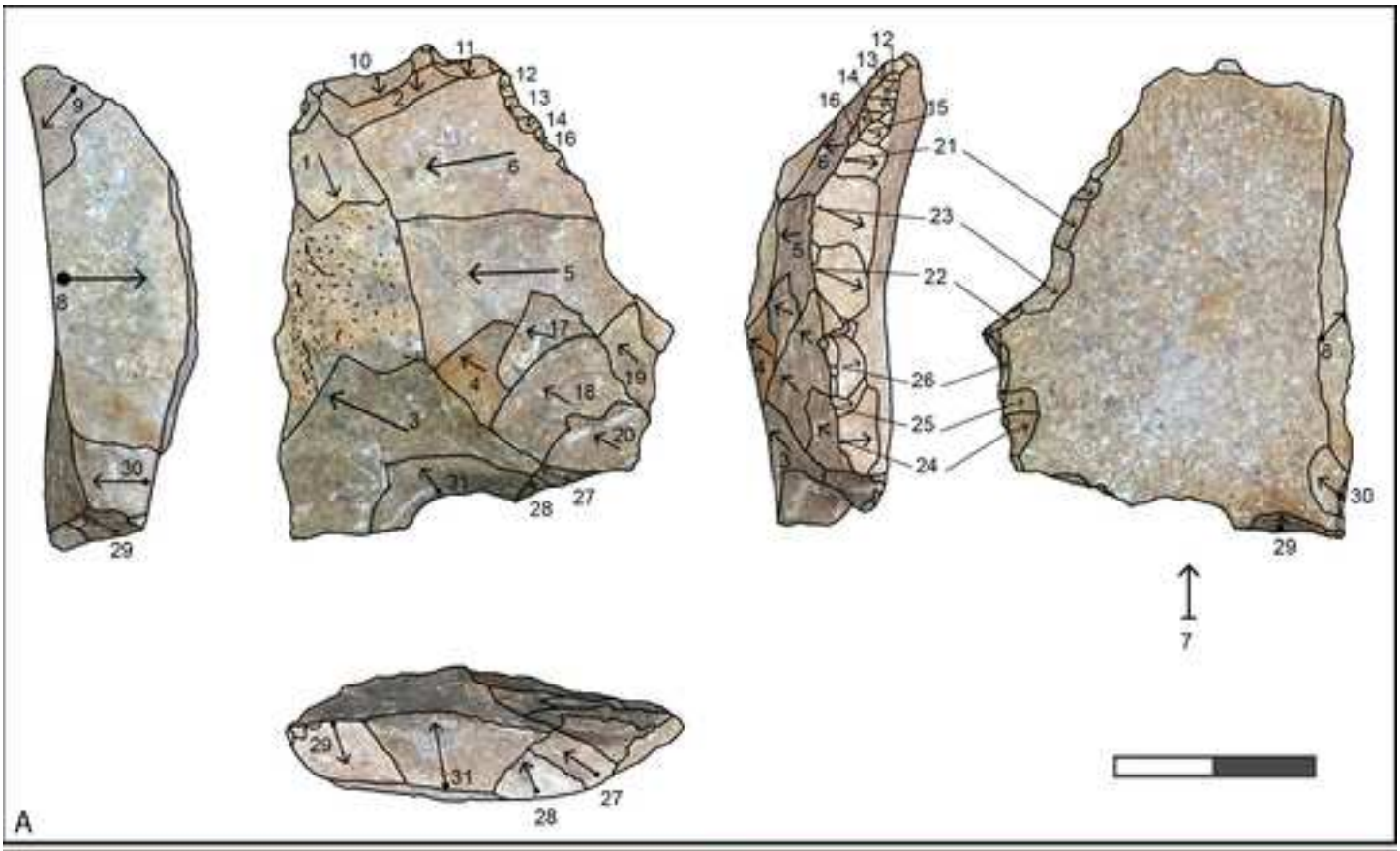

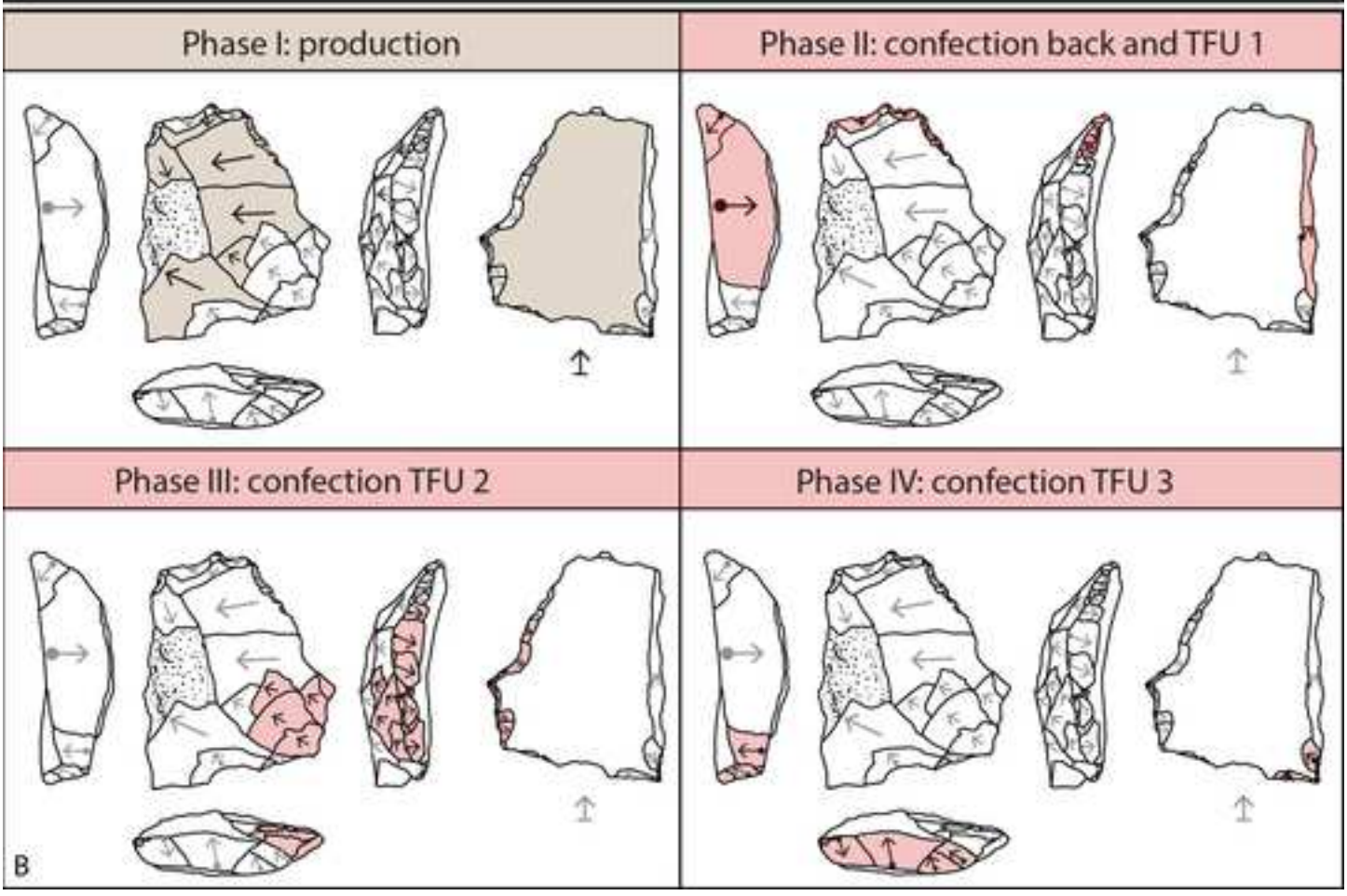

Figure 14

Click here to access/download;Figure;FIG14.jpg

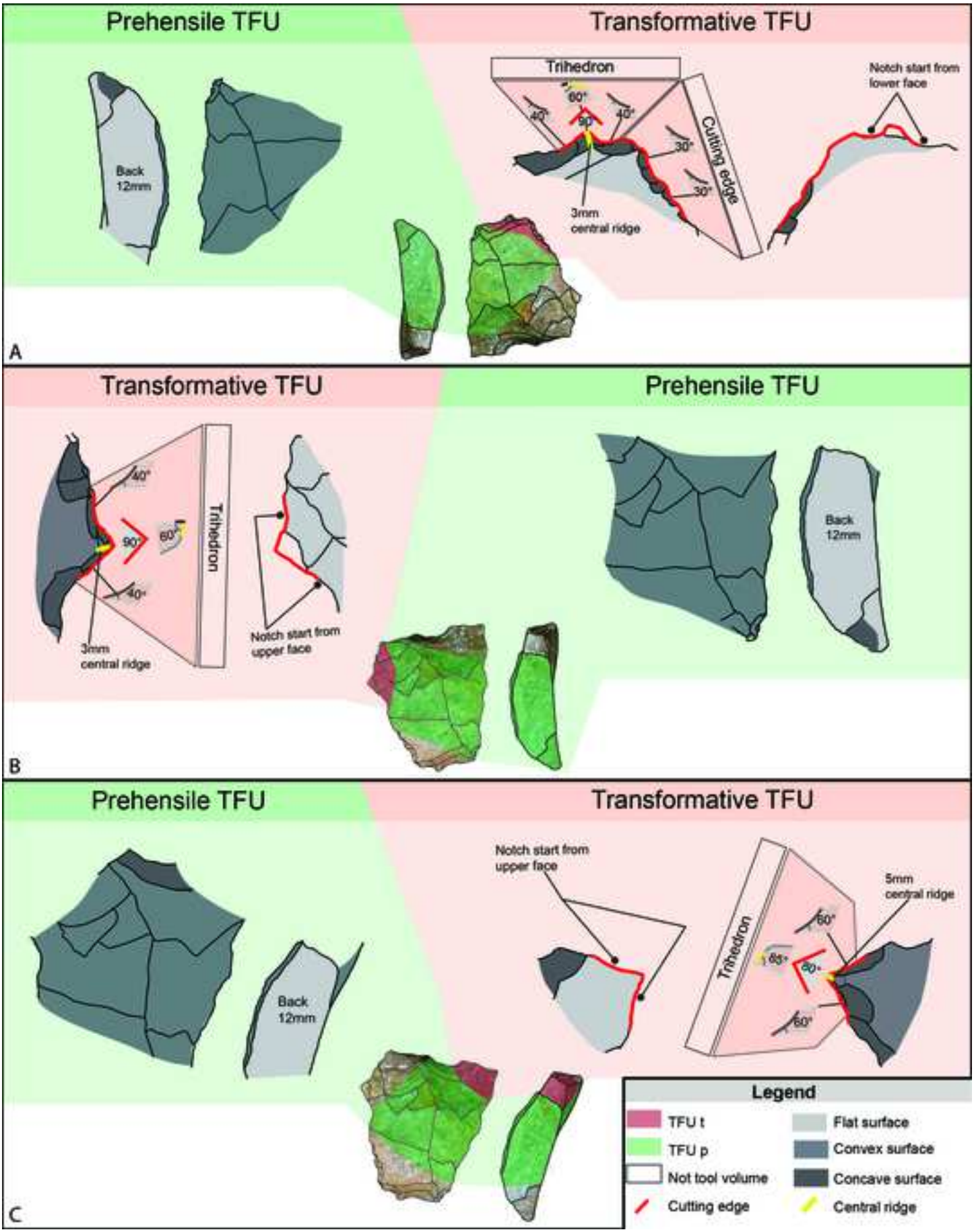

Figure 15

Click here to access/download;Figure;FIG15.jpg

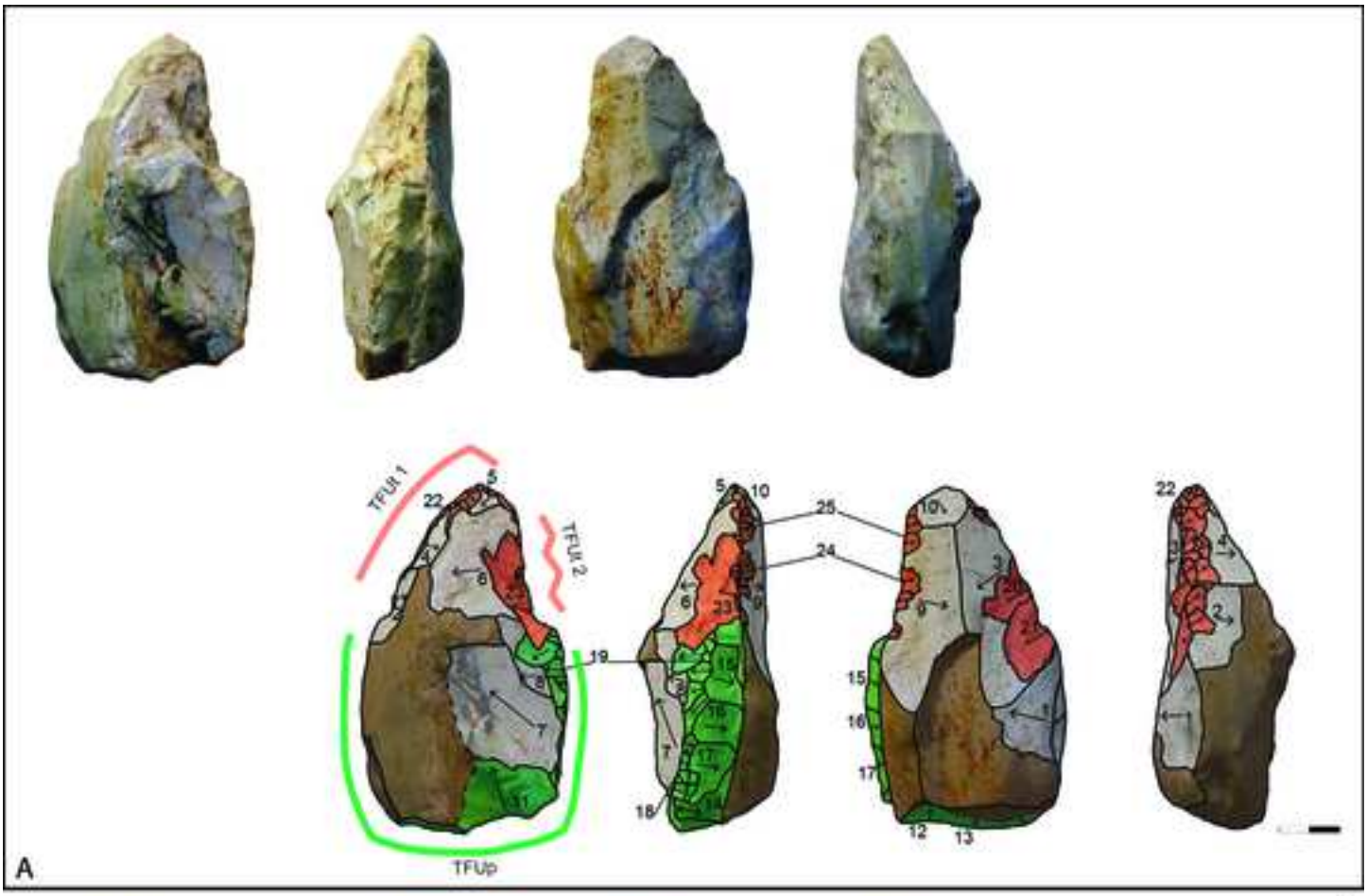

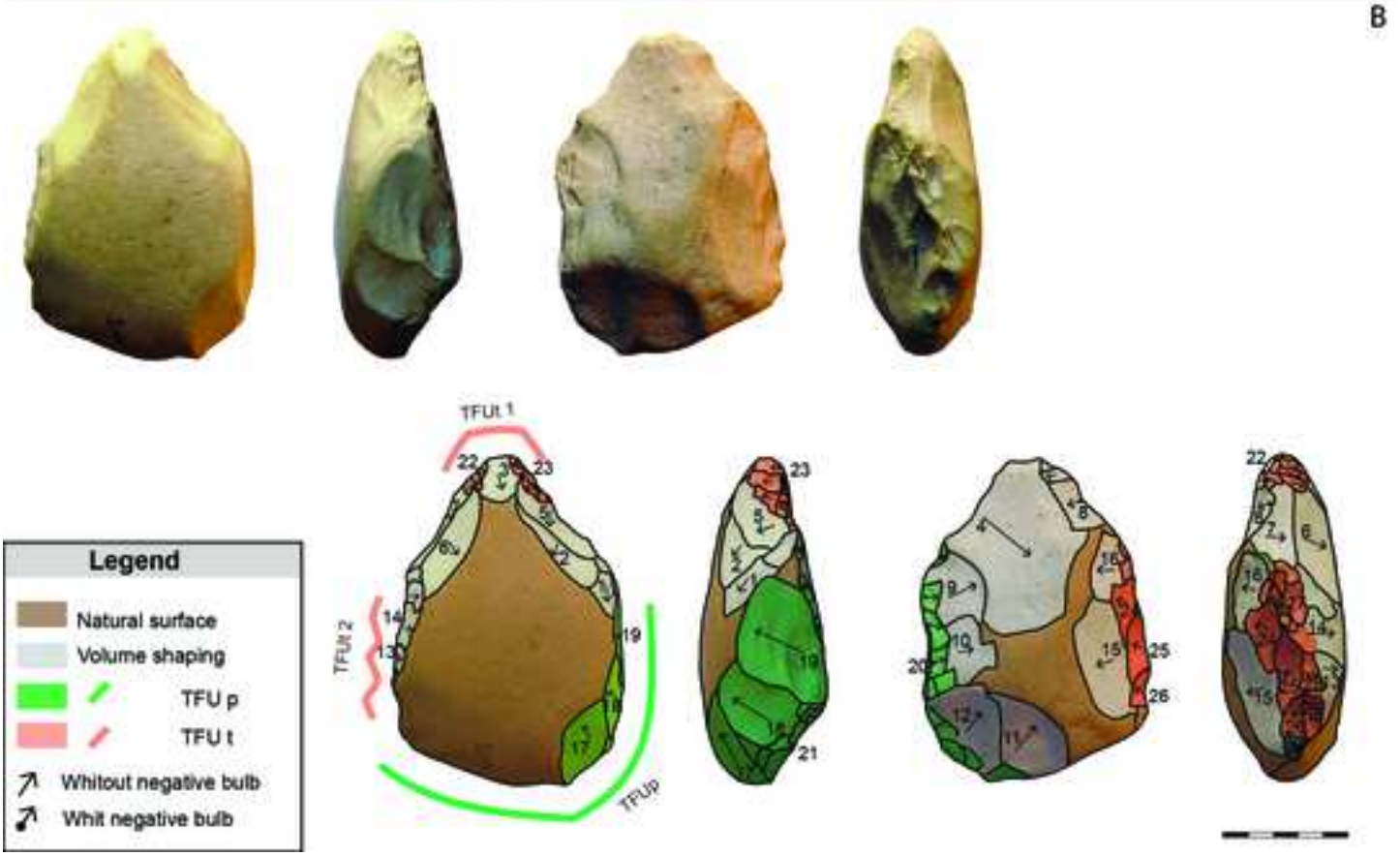

Stratigraphic units						Radiometric age by Villa and Buettner, 2009 (Ma)
Supersynthem	Synthem	Subsynthem	Units code	Brief description of lithology and deposit interpretation	Thickness (m)	
MONTICCHIO	**Laghi di Monticchio**	Serra di Braida	LGM5	Alternating beds of massive (fall deposits) to cross-laminated (pyroclastic surge) tuff and lapilli stone.	4 - 5	
		Lago Piccolo	LGM4	Alternating beds (cm-thick) of massive to cross-laminated tuff and lapilli stone (pyroclastic surge).	5	**0.141±11**
		Lago Grande	LGM3	Massive (fall deposits) to cross-laminated (pyroclastic surge) tuff with scattered blocks (cm to m-sized).	5	
		Piano Comune	LGM2	Fine to coarse-grained parallel laminated tuff locally with pisolites and cross-laminations (pyroclastic surge).	7	
		Casa Rossa	LGM1	Volcanic breccia deposit covered by fine-grained, cross-laminated tuff (pyroclastic surge).	1-5	
	Valle dei Grigi – Fosso del Corbo	Masseria di Cuscito	VGC3	Fine-grained cross-laminated tuff (pyroclastic surge) cut by an erosive surface and covered by two massive breccia deposits (pyroclastic flow).	7	
		Imbandina	VGC2	Massive beds of tuff and blocks (pyroclastic flow) with subordinate fine-grained cross-laminated tuff (pyroclastic surge); 4-m-thick clast-supported, coarse-grained, sedimentary and lava blocks bearing lapilli tuffs unconformably lie on the previous unit and underlie in turn 1-m-thick welded, agglutinated lapilli tuff (carbonatite).	8	
		Case Lopes	VGC1	Breccia deposits and thick beds of fine- to coarse-grained tuff, with cross-lamination (pyroclastic surge); at the base, a 4-m-thick black scoriae (basanite) is present.	15	0.530±22 **0.494±5**
MONTE VULTURE	**Melfi**	Solagne - Arcidiaconata	SMF4	Travertine deposits.	4-5	
		Piano di Croce	SMF3	Lava flow (haüynitite), covered by 3-m-thick massive to cross-bedded tuff (pyroclastic surge).	6	
		Castello di Melfi	SMF2	Dark-grey lava flow ("Melfi haüynophyre" *auctt.*),	1 to 20	0.573±4
		Gaudo	SMF1	Epiclastic volcanic alluvial conglomerates, with rare intercalations of sands, laterally heteropic to swamp sediments.	12	
	Barile	Ventaruolo	SBL4	Dark-grey-green pumice fall deposit, in dm-sized layers alternated with massive yellow tuff with blocks (pyroclastic flow), yellow tuff with accretionary lapilli (fall deposits) and yellow to red cross-bedded tuff (pyroclastic surge).	1.5-8	<0,610
		Vulture – San Michele	SBL3	Massive deposits (10-15 m thick) of tuff with dm-sized heterolithologic blocks (pyroclastic flow), alternated with: i) levels of pumices (fallout deposits), ii) lava flow (foidites, tephro-foidites, tephrites, basanites); these units are laterally correlated with epiclastic volcanic conglomerates, sands, and massive pelites (alluvial and lacustrine deposits).	500	0.609±9 0.611±6
		Rionero	SBL2	Composed of three lithofacies. The lowermost lithofacies is made of massive dm-thick beds of pale-yellow fine-grained tuff (fall deposits) with horizons of accretionary lapilli and m-thick beds of fine-grained, cross-bedded tuff with lenses bearing cm-sized white pumices (pyroclastic surge); the intermediate lithofacies is made of lapilli fallout (thephrite, foidites) alternated with dm-sized massive or trough cross-beds of yellowish tuff (pyroclastic flow); the uppermost lithofacies is constituted of massive proximal fall and surge deposits, with m-sized ballistic lava blocks. In the Atella and Venosa basins, the volcanic succession is heteropic to lacustrine and alluvial deposits).	44	0.630±20 0.672±6 0.714±18 <0.720±15
		Toppo San Paolo	SBL1	Pale gray lava dome (haüyne phonolite).	140	0.673±19
	Foggianello	Fara d'Olivo	FGG3	Composed of two ignimbrite units, both made of massive to planar cross-bedded tuff with sparse cm-sized pumices (trachyphonolite) and rare lithics (pyroclastic flow deposits).	10	Upper ignimbrite <0.755±21; <0.781±29 Lower ignimbrite 0.742±22; 0.737±16
		Campanile	FGG2	Sequence of massive (fall deposits) and subordinate cross-bedded (pyroclastic surge) tuff.	3-4	
		Spinoritola	FGG1	Alluvial conglomerate with subordinate lava clast of the Spinoritola dikes (haüina-trachyte composition).	25-30	0.698±25; 0.698±48; 0.678±9; **0.698±8**

Table 1: Description of the Monte Vulture Volcano stratigraphic units (after Giannandrea et al., 2004, 2006, and Stoppa et al., 2008). Unit codes correspond to those of the official 1:50,000-scale geological sheet (Foglio 451 Melfi, Carta Geologica d'Italia, 2010

Table 2: List of pyroclastic and epiclastic lithofacies with a brief description and interpretation

Facies code	Facies	Sedimentary structures	Interpretation
Bmli	Poorly-sorted matrix-supported epiclastic volcanic breccia, with lithic industry. Angular to sub-angular pebbles ranging in size from 1 to 10 cm. Matrix consists of grey middle- to coarse-grained epiclastic volcanic sandstone.	Structureless/massive beds	Cohesive debris flows deposits
Suli	Epiclastic volcanic sandstone, with volcanic angular to sub-angular pebble (ranging in size from 1 to 10 cm) and lithic industry.	Poorly-defined undulated beds	Reworked colluvium
SBt	Coarse epiclastic volcanic sandstone and angular to sub-rounded epiclastic volcanic clast-supported breccia, with scattered cobbles (10-50 cm size).	Trough cross-beds	Channel infill by water stream flow of the reworked volcanic fallout and pyroclastic flow deposits
Sr	Gray fine-grained epiclastic volcanic sandstone.	Ripple cross-lamination	Ripples (lower flow regime)
Sh	Light grey epiclastic volcanic siltstone.	Horizontally thinly laminated	Decantation, lake deposits.
Dh	White to light-grey silty-clay diatomites.	1-15-cm-thick massive to laminated beds	Shallow-lake deposits
Su	Red siltstone.	Massive appearance or with poorly defined planar lamination in undulated beds	Hydrothermal alteration of volcanic material
TLBm	Medium- to coarse-grained tuff with fine- to coarse-grained angular lapilli stones and blocks (max 27 cm size).	Structureless/massive beds	Pyroclastic debris flows
LTm	Fine- to coarse-grained lapilli stone, with medium-grained tuff. Presence of some angular blocks max 10 cm size.	Structureless/massive beds	Pyroclastic debris flows
Lm	Coarse-grained clast-supported lapilli stone with grey pumice.	Structureless/massive beds	Lapilli fallout deposits
TLm	Grey fine- to coarse-grained tuff with fine-grained scattered lapilli, locally covered by 1-3-cm-thick light-grey fine-grained tuff.	Massive appearance or with poorly-defined planar lamination	Lower-concentration pyroclastic currents and co-current falls
Tng	Grey fine- to medium-grained tuff.	Normal grading	Decantation of a volcanic fall deposit in shallow fresh water
Tm	Fine- to coarse-grained tuff.	Structureless/massive or poorly-defined laminated beds	Fallout deposits

Table 3:ESR data and ages obtained for Atella samples.

Level	^{238}U (ppm)	^{232}Th (ppm)	K (%)	D_α (µGy/a)	D_β (µGy/a)	$D_{\gamma+cosmic}$ (µGy/a)
L3	7.09± 0.15	20.19 ± 0.28	1.35 ± 0.02	179 ± 3	2083 ± 32	2018 ± 102
L1	4.44 ± 0.17	18.37 ± 0.32	1.19 ± 0.02	138 ± 4	1652 ± 38	2375 ± 110

Level	Used center	Bl max. (%)	W (%)	D_e (Gy)	D_a (µGy/a)	Ages (ka)	Mean Ages (ka)
L3	Al	51	10 ± 5	1870 ± 100	4297 ± 111	435 ± 23	442 ± 39
	Ti -Li	100		1990 ± 175		463 ± 41	
L1	Al	53	10 ± 5	2134 ± 159	4147 ± 121	515 ± 39	509 ± 56
	Ti -Li	100		2081 ± 175		502 ± 42	

Table 4: Number of archaeological finds

Levels	Old excavation (Borzatti)	New excavation (EFR)	Total
L complex	107	0	107
F complex	667	*Deb 1: 261* *Deb 2: 129* 273	940
Total	774	273	1047

Table 5: Distribution of lithic artefacts by technological category. Retouch flakes and flakes from shaping small tools: small retouch flakes, notch flakes, small flakes from shaping the edges of small tools; Small tools: entire and fragmented small tools; Core: entire core and fragment of core; Flakes: production flakes from a flaking reduction sequence; Large tools: Handaxes and large shaped tools; Indet: debris, indeterminate small fragment, chunks.

Technological categories	Retouch and small tool-shaping flakes	Small tools	Cores	Flakes	Large tools	Indet	Total
Level L	46	16	2	15	0	28	107
Level F	222	250	23	386	28	31	940
Total	268	266	25	401	28	59	1047

Table 6: Size of faunal specimens in the whole site

Size	TOT	TOT %
1 cm	54	9.2
2 cm	131	22.4
3 cm	116	19.8
4 cm	108	18.5
5 cm	67	11.5
6 cm	29	5.0
7 cm	20	3.4
8 cm	11	1.9
9 cm	7	1.2
10 cm	9	1.5
11 cm	4	0.7
12 cm	5	0.9
13 cm	3	0.5
14 cm	3	0.5
15 cm	5	0.9
16 cm	0	0.0
17 cm	3	0.5

18 cm	2	0.3
19 cm	2	0.3
20 cm	1	0.2
21 cm	1	0.2
25 cm	0	0.0
28 cm	1	0.2
30 cm	3	0.5
TOT	585	100

Table 7: Alteration of fragments

	F	**H**	**L**
Rounded fragments	38.5	43.4	7.1
Slightly rounded edges	22.3	22.6	18.8
Not altered	39.2	34.0	74.1
TOT	462	53	85

Table 8: Taxonomy of faunal remains per level

	Levels					
Taxon	F	G	G/H	H	L	M
Bovinae indet.	9	0	0	0	3	0
Bovid/Cervid	1	0	0	0	1	0
Caprine	0	0	0	1	0	0
Cervus elaphus	10	0	0	2	7	0
Dama sp.	0	0	0	1	3	0
Cervid	19	0	0	1	6	0
Ungulate	9	0	0	3	3	0
Palaeoloxodon antiquus	24	0	0	1	3	0
Palaeoloxodon size	11	0	0	0	5	0
Unidentified	385	2	9	45	54	1
Small mammal	1	0	0	0	0	0
Testudines	0	0	0	1	0	0
TOT	469	2	9	55	85	1

Declaration of interests

☒ The authors declare that they have no known competing financial interests or personal relationships that could have appeared to influence the work reported in this paper.

☐The authors declare the following financial interests/personal relationships which may be considered as potential competing interests: